NORTHWESTERN UNIVERSITY

Crack Response of a Historic Structure to Weather Effects and Construction Vibrations

A Thesis

Submitted to the Graduate School In Partial Fulfillment of the Requirements

For the Degree

MASTER OF SCIENCE

Field of Civil Engineering

By

REMI BAILLOT

EVANSTON, IL

December 2004

Table of Contents

Acknowledgments

This thesis is the achievement of many hands and minds that deserve more than simple acknowledgment. The long-term relationship between my French engineering school in Paris, l'ESTP, and Northwestern University is contributing to excellent academic opportunities; I thank these two institutions for their early understanding of the rewards the relationship provides.

My advisor Professor Charles Dowding is warmly thanked for his guidance, expertise, motivation and unique taste for research, without which my masters thesis at Northwestern would certainly not have been born. I am also grateful to Professor Dowding for the good relationship we maintained throughout my stay at Northwestern.

Thanks are also given to Professors Finno and Dowding for their geotechnical instruction. Thank you to all the graduate students of the geotech lab, and a special thanks to my Galatasaray's fan, Hasan Ozer, for his priceless help, patience, advice and support since the beginning. Good luck to Brandon who just started.

I am indebted to the Infrastructure Technology Institute for funding my research, and most of all to the ITI staff, in particular to Dan Hogan, Daniel Marron, David Kosnik and Matthew Kotowsky for their excellent technical support and friendly moments in the windowless ITI lab.

This project was made possible through the cooperation of the Eastern Federal Lands Division of FHWA, the Department of State and Parsons Brinkerhoff Quade and Douglas. Special thanks are given to James Chapman of the Department of State, Jorge Alvarez of FHWA, George Kanelos of GSA, and Douglas Anderson and Robert Kalbach of PBQD.

Thanks to Emilie, Franck and Erica for their strong support and all that I can't say here; to "Le P'tit" for his chores and mouth sound effects; to Aalia and the "Indian house" on Garnett; and to the mixture of Beethoven, Satie, The Smashing Pumpkins, Mozart, Chopin, Daft Punk, Muse, Nirvana, Bach, The Pink Floyd, Rostropovich, The Doors, Air, The Red Hot Chili Peppers, Noir Desir, The Chemical Brothers, Pearl Jam, Dido, The Beatles, Aerosmith, Vivaldi, The Buena Vista Social Club, Ugly Kid Joe, Rachmaninov, Ben Harper, Bebel Gilberto, Eric Clapton, Supertramp, Dire Straits, Bob Marley etc… for helping me during the long and cold nights by the candle, writing this thesis.

Very special thanks to my uncle Philippe, and to my Grandma who will always be in my heart.

A mon père et au petit qui va naître.

Abstract

Cosmetic cracks are very common in structures, and most of the time they remain unnoticed and do not decrease the structural integrity. Although these cracks are unremarkable and barely noticeable, occupants become concerned about these cracks when construction occurs nearby. In order to investigate the true nature of these cracks, the Automated Crack Monitoring (ACM) was developed. It allows the simultaneous measurement of crack responses to environmental changes and vibrations induced by various construction activities. While vibration environment is defined by seismological transducers, the ACM dual-purpose crack displacement sensors measure crack response.

This thesis involves an ACM study to compare construction vibration, human household activity and long-term weather effects on a historical building in downtown Washington DC. Measurements and analysis show that construction activity in the vicinity of the structure did not create significant ground motion; long-term environmental crack displacement was 20 to 60 times greater than that caused by the largest measured construction-induced ground motion; crack displacements produced by occupant activity were larger than the largest construction vibration-induced crack displacement by a factor of 2 to 16, but smaller than the long-term environmental or weather induced crack displacement; and exterior cracks experienced larger weather-induced displacements than either of the two interior cracks.

LIST OF FIGURES

LIST OF TABLES

CHAPTER 1

Introduction

This thesis analyzes micrometer crack expansion and contraction response to construction-induced ground motion at a historical building in downtown Washington DC. This structure was instrumented, and its response was studied as part of the development of an Autonomous Crack Measurement (ACM) system sponsored by the Infrastructure Technology Institute at Northwestern University through a grant from the United States Department of Transportation. Autonomous Crack Measurement (ACM) is an automated measurement system developed in order to compare micrometer displacement of cosmetic cracks in structures produced by long-term weather effects to those produced by construction effects and human activity.

Crack responses in the Washington D.C structure were measured with Kaman eddy current sensors, while ground motions were measured in the three orthogonal axes in front of the house with standard vibration monitoring geophone transducers. Three cracks were monitored, one external on the building façade stucco and two internal between two pieces of molding and in the plaster and lath above a door frame.

This thesis also presents background for a "Donut LVDT qualification test" in Appendix A to determine the reliability and testing performances of LVDT crack displacement sensors. This investigation was conducted to develop a simple method to qualify micrometer measurement systems before they are employed on site since ACM

performances are directly dependent on this sensor accuracy. Conclusions regarding this qualification test are presented separately in the end of Appendix A.

This thesis is divided into five chapters. Chapter 2 presents the construction environment and the external and internal instrumentation. The chapter includes a description of the structure and location of the instruments, an explanation of the construction goal and equipment, and discussion of the slight degradation resulting from sensor removal.

Chapter 3 is a discussion of the long-term weather effects and occupant activity on crack displacements. It contains a description of the corrected crack response and of the 24-hour rolling average, long-term crack responses to environmental effects, a summary of the three maximum weather descriptors, and the occupant activity responses of the two interior cracks.

Chapter 4 presents the measurement and analysis of construction equipment-induced vibration response. It includes consideration of data acquisition, triggering mechanisms, and the challenges presented by construction monitoring; the ground motion environment; a description of "noise" events; ground motions and crack displacements resulting from construction activities of a backhoe and a jackhammer; comparison of occupant induced and jackhammer-induced crack displacements; comparison of response to a door slam and long-term cyclic weather effects.

Chapter 5 summarizes the conclusions.

CHAPTER 2

Construction Environment and Instrumentation

Introduction

Road construction immediately in front of the historic structure shown in Figure 2-1 led to concern over possible cracking. Midway though the project the Autonomous Crack Measurement system was installed as a means of determining the effect of construction induced vibrations. The ACM system was in place for three months from July to October while utilities in the sidewalk were replaced and the roadway surface was repaved.

Figure 2-1: Front view of the façade of the instrumented house.

Construction

Construction goal

The instrumented structure was located on a major thoroughfare undergoing reconstruction including utility replacement. The two other upper photographs in Figure 2-2 were taken at the end of July 2004, in the middle of the project. The upper right photograph shows the original brick sidewalk and the beginning of a trench to exhume and replace existing utilities. The bottom two photographs were taken mid October 2004, when the project was close to its end, and the final paved surface was in place.

Figure 2-2: Views of street a) during (upper) and b) after (lower) reconstruction.

Construction equipment

Reconstruction activities during the period of observation included the excavation of a 1-meter wide trench several meters from the façade of the house. The four photographs in Figure 2-3 show details of the excavation. As shown in the upper two photographs, trenching was performed in front of the house around the 24th of July 2004 by backhoe. Jackhammers were also in use very close to the house by the end of the construction.

The house was not instrumented during the initial stages of the project during removal of more distant utilities and structures in the middle of the street.

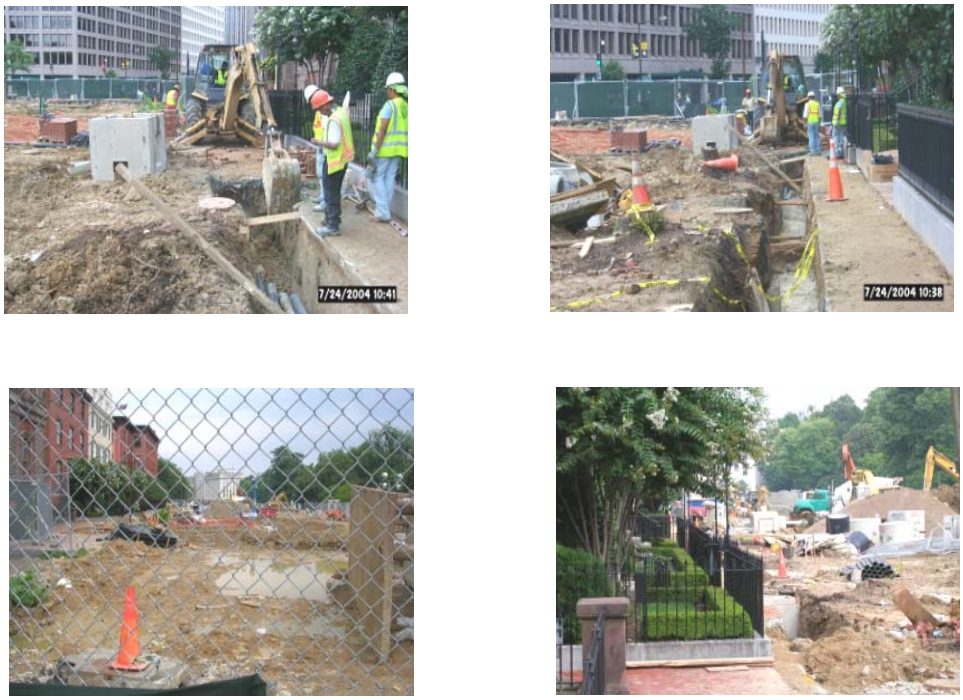

Figure 2-3: Trenching activities within two meters of the structure.

Instrumentation

As shown in Figure 2-4, the structure was instrumented with a geophone to record ground motion and 3 sets of sensors to measure changes in crack width. Figure 2-4 shows both the plan location of the instruments (Figure 2-4 a, upper) and the elevation location of the instruments and wiring (Figure 2-4 b, lower). Details of the location of the geophone and crack sensors are shown in Figure 2-5. Each instrument is graphically described by a large scale location and a small scale detail photograph, which are related by the red colors and boxes.

The tri-axial geophone was buried in garden soil half a meter away from the house, toward the street. It measured ground motion excitation in three mutually perpendicular directions, longitudinal, transverse and vertical. To remain consistent with former studies, the longitudinal axis was defined as parallel to the long axis of the structure, and in this case parallel to the street.

Cracks were instrumented with Kaman sensors, which are capable of measuring crack displacements of as little as 0.1 μm or 4 μin. All crack sensors were in place from the 16th of June 2004 and to the 15th of October 2004. Sensor recordings were obtained on an intermittent basis until the 19th of July. Before the 19th of July there was insignificant construction activity and telecommunication was not fully functional, so this information is not included here.

In the interior two cracks were monitored: the joint between two components of the floor molding (2nd floor-crack 2) and a crack in the wall above a door frame (3rd floor,

crack 3). Location and detail photographs are shown in Figure 2-5. The external monitored crack was located in the stucco façade facing and closest to the construction.

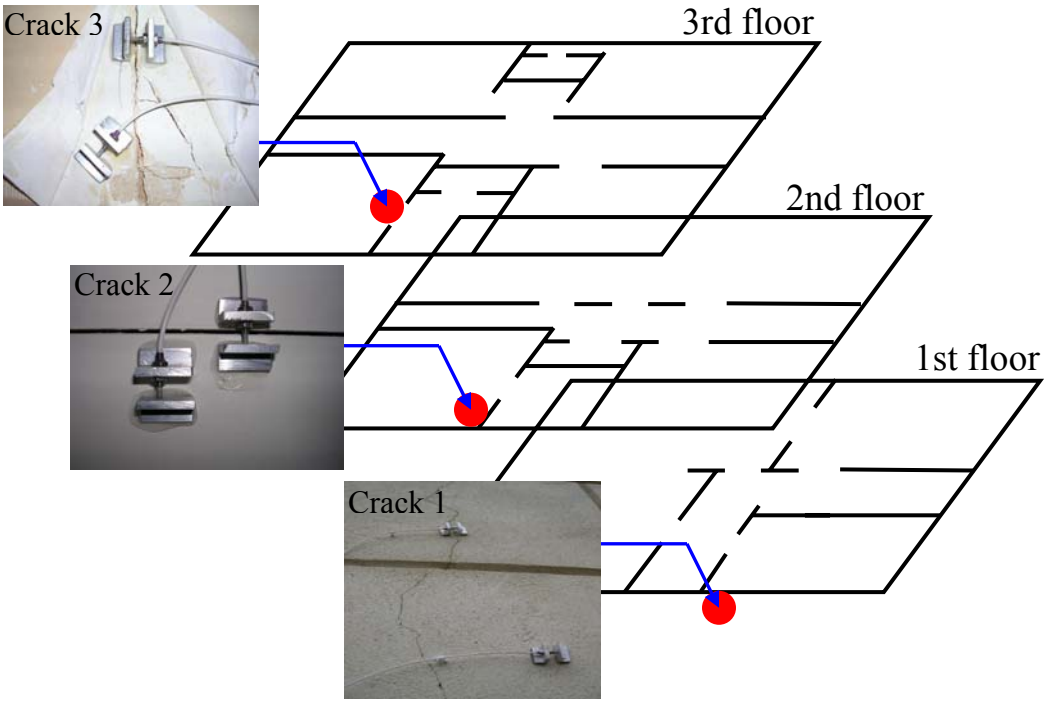

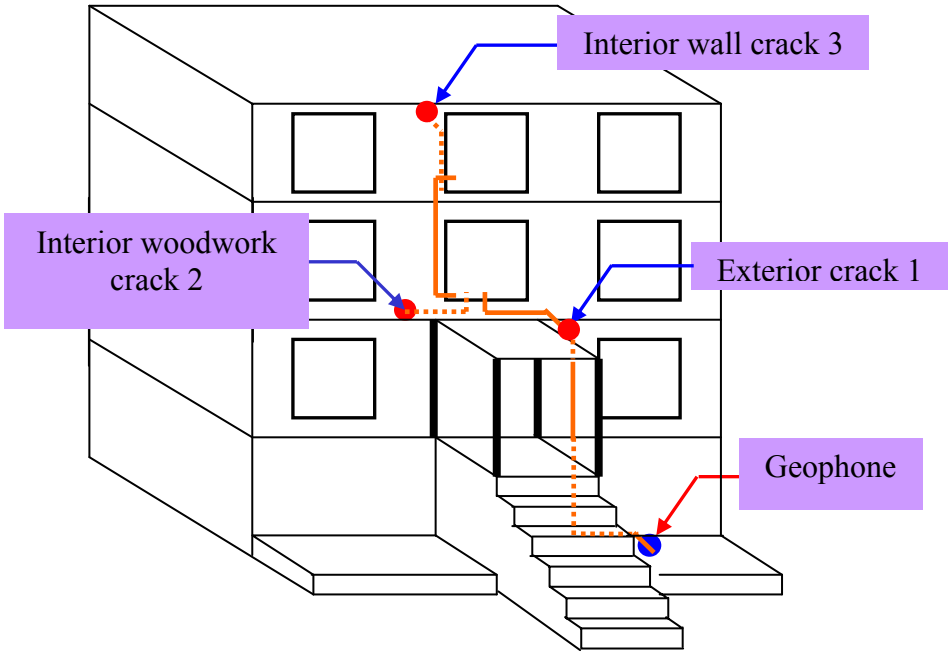

Figure 2-4: Three dimensional view of the instrumentation: a) (upper) expanded views of floors with x,y locations and b) isometric view with z locations.

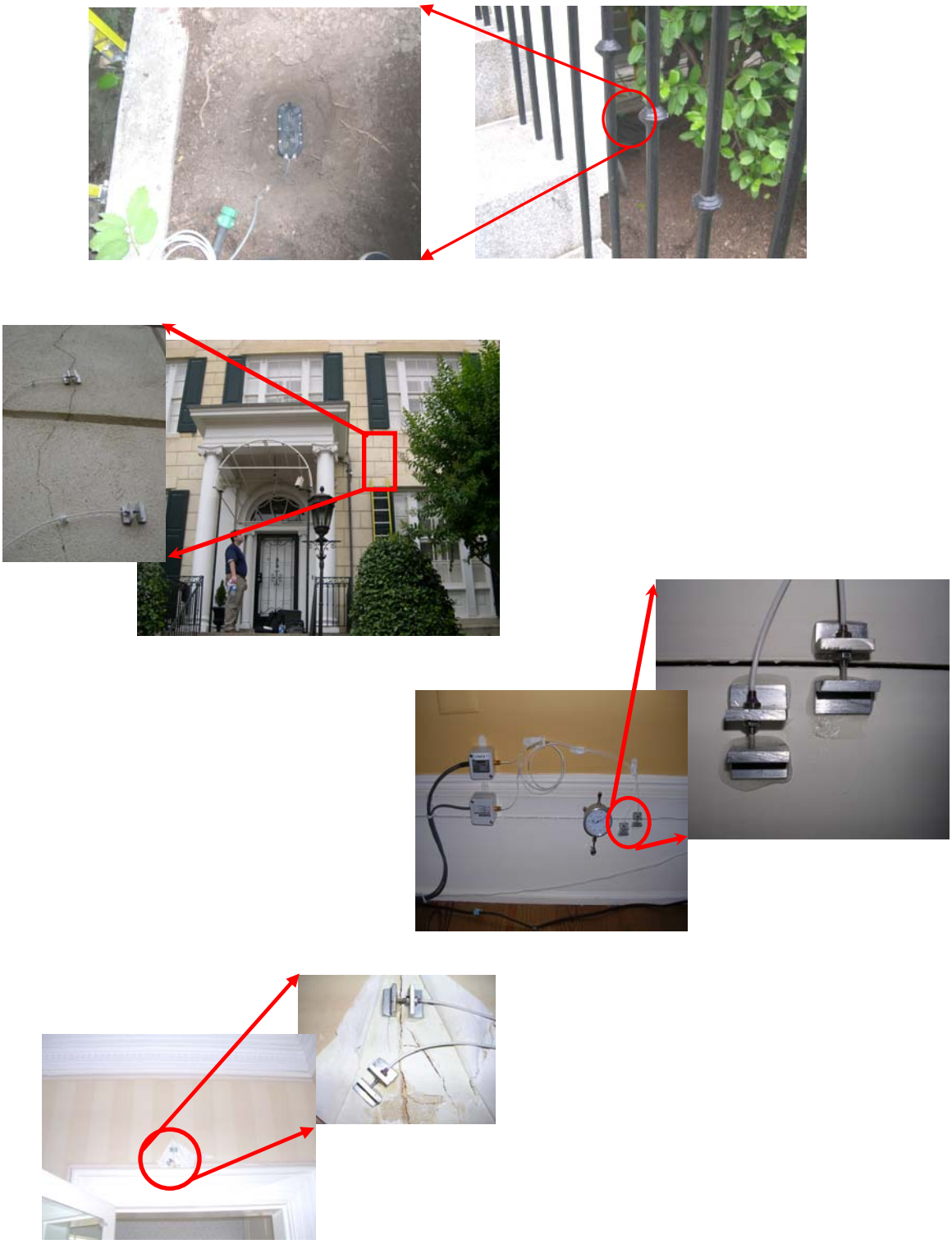

Figure 2-5: Photographs showing the location and details of the geophone and three cracks, whose long term and dynamic response was monitored.

Each crack sensor is accompanied with a null sensor to zero out sensor and wall material response to changes in temperature and humidity. Null sensors are placed on uncracked material adjacent to the crack being monitored. Null sensor response is subtracted from the crack sensor response to obtain the crack response itself.

Vaisala weather loggers recorded temperature and humidity hourly, both internally (HMW40/50) and externally (HMW61/71). Measurement ranges were chosen to match the internal and external conditions. Locations of the weather loggers are shown in Figure 2-6: the external logger was located above the portico on the second floor and the internal logger was placed in the same room as crack 2.

Figure 2-6: a) external and b) internal weather loggers.

All of the three crack sensors and their null sensors, as well as the geophone and weather loggers were wired to the eDAQ data acquisition system shown in Figure 2-7. This data acquisition system enables recording of dynamic (transient) and long-term

(weather) response from all three cracks. Crack sensors acquire transient response whenever the vibration level at the outside geophone exceeds a predetermined excitation or trigger threshold. Environmental or long-term response is obtained with readings collected every hour. In addition an index of the general vibration environment is obtained with geophone readings every minute. This ground motion environment measurement allows tracking of general activity levels to be recorded whereas the trigger mechanism captures peak events. Some 13 instruments were wired to the eDAQ: 3 geophones (one for each axis), 3 null sensors, 3 crack sensors, 2 temperature and 2 humidity sensors.

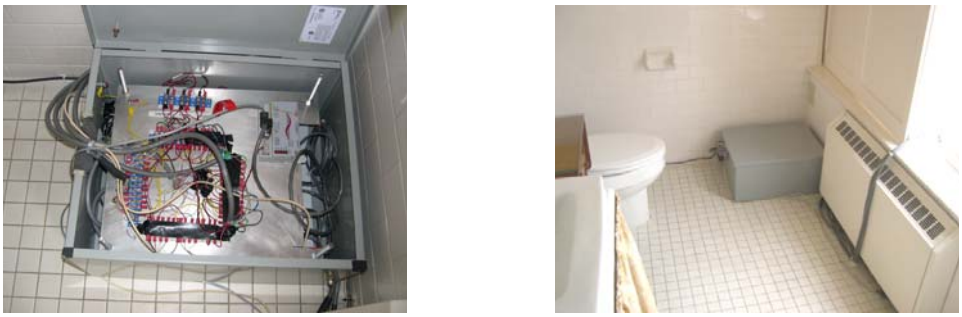

Figure 2-7: Data logger and junction box installed on second floor.

Removal of the instruments

The removal of the Kaman sensors, humidity and temperature sensors inside and outside caused insignificant degradation to the building. The 5 pairs of photographs in Figure 2-8 show respectively on the left and right side the state before and after the removal for the three cracks, cable harness, and finally four brackets after they were removed from the outside stucco and inside wall plaster. Although the sensor bracket

mounts were epoxied to the walls, only small amounts of plaster or stucco remained on the brackets. Scuffing of the painted surface of the molding was even less.

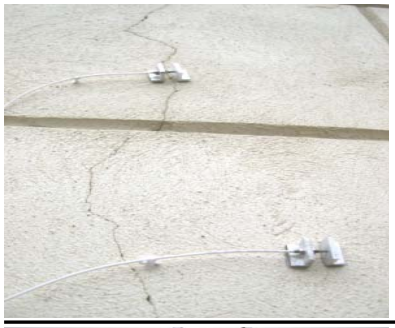


exterior stucco crack 1

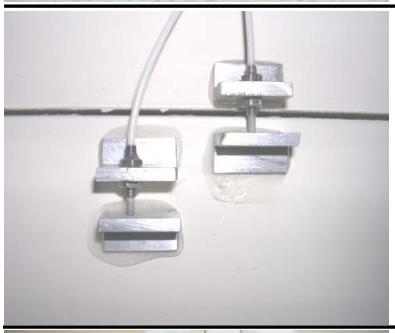


interior molding joint crack 2


interior plaster and lath crack 3

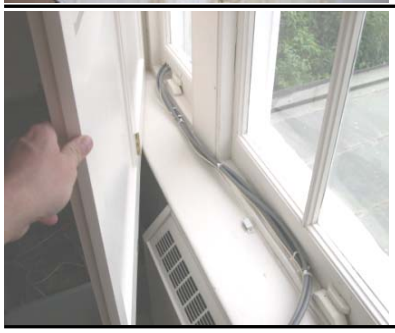


wire harness


kaman brackets

Figure 2-8: Before and after comparisons of insignificant degradation caused by removal of the instruments.

CHAPTER 3

Weather and Occupant activity

Introduction

Response of the cracks to weather and human activity provides the background crack response against which vibration response should be compared. Both weather and habilitation effects are discussed in this chapter, and both are significant as has been found in other studies (Siebert (2000), McKenna (2002), Snider (2003)). Crack response caused by changes in the weather will be discussed first.

Weather effects are obtained by measuring the crack width each hour and then plotting that response over time as shown in Figure 3-1. Herein changes in crack width will be called crack "displacement" to simplify the term and to follow terminology in other reports. Figure 3-1a shows 3 curves crack, null and corrected displacement. This 3 day time period shows only a daily temperature induced change.

Long-Term Weather Response

Corrected Crack response from the Null and Crack responses

Null sensor readings are subtracted from crack sensor readings as shown in Figure 3-1. Displacements measured by the null sensor are due principally to temperature variations, which tend to expand and contract the metal of the sensor and the wall material. As this same phenomenon occurs for both null and crack sensors, the null sensor displacements are subtracted from the crack sensor displacements to obtain the "corrected displacements" which are those of the crack itself. As the graph shows, the "corrected displacements" are somewhat larger than the crack displacements by a few micrometers. All the following graphs are plotted with the correction mentioned above, therefore "crack response " will explicitly mean "corrected crack response" for a question of simplicity.

Once the crack response obtained, the 24 hour rolling average is calculated and plotted as shown in Figure 3-1 b (lower). The 24-hour average was systematically calculated at each hourly measurement by averaging the data 12 hours before and 12 hours after each individual sample. See McKenna (2002) for details. The 24-hour rolling average has been calculated for responses of the all three cracks as well as exterior and interior temperature and humidity in the same manner.

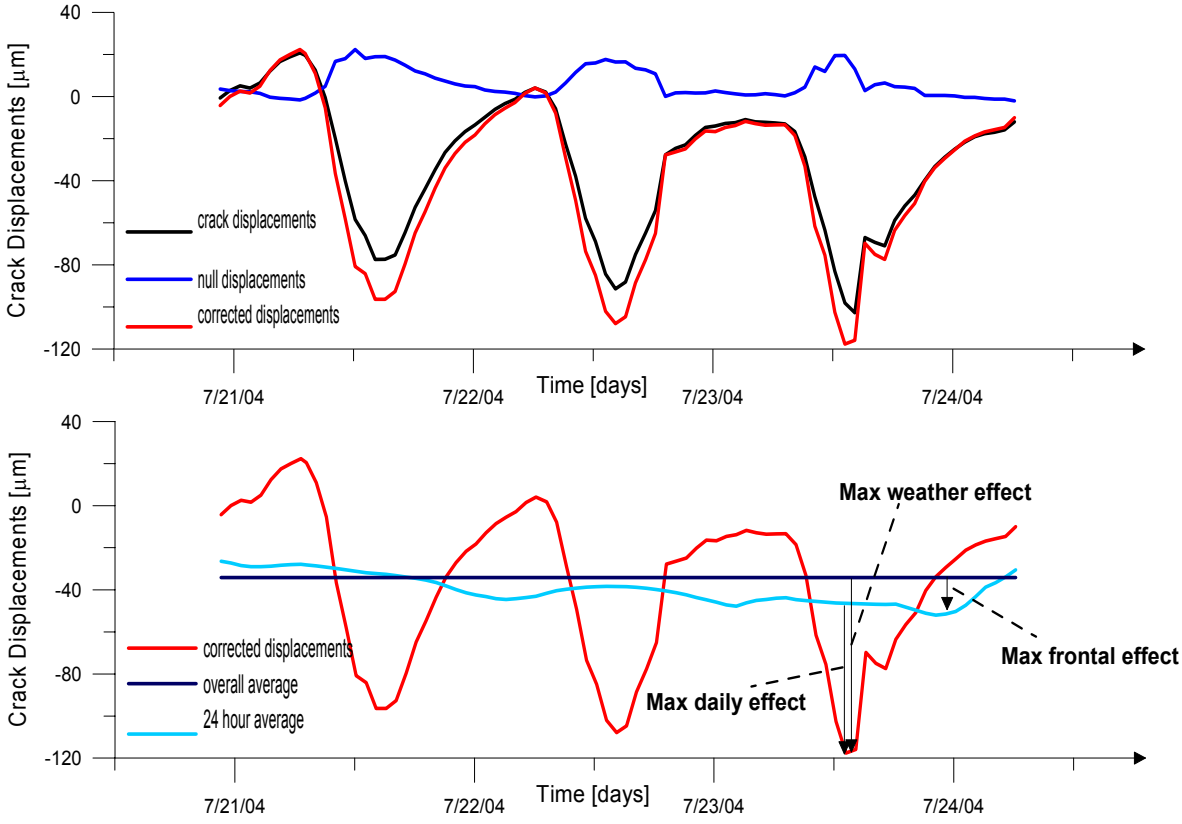

Figure 3-1: Typical crack displacements a) null correction b) weather descriptors and 24-hour average.

The maximum frontal effect is defined as the absolute largest deviation between the 24-hour rolling average (blue) and the overall average (horizontal purple), which is the average of the field measurements over the full time-period. The frontal effect is shown by the farthest right vertical arrow. The maximum daily effect is defined as the absolute largest deviation between the 24-hour rolling average and the maximum field measurement. The last descriptor is the maximum weather effect (the largest vertical

arrow), or in other words the gap between the overall average and the maximum field measurement.

Figure 3-2 compares long-term crack response with long-term weather indicators for the exterior crack for a longer period (12 days). It compares long-term outdoor crack 1 changes to outdoor temperature and humidity. Temperature, humidity and crack displacement are always plotted on the same time-scale for graphical comparison. The red curve represents the field measurements whereas the black curve is the 24-hour average. This 12 day period shows both the daily responses as well as the passage of the weather front at the end (5 through 10 August).

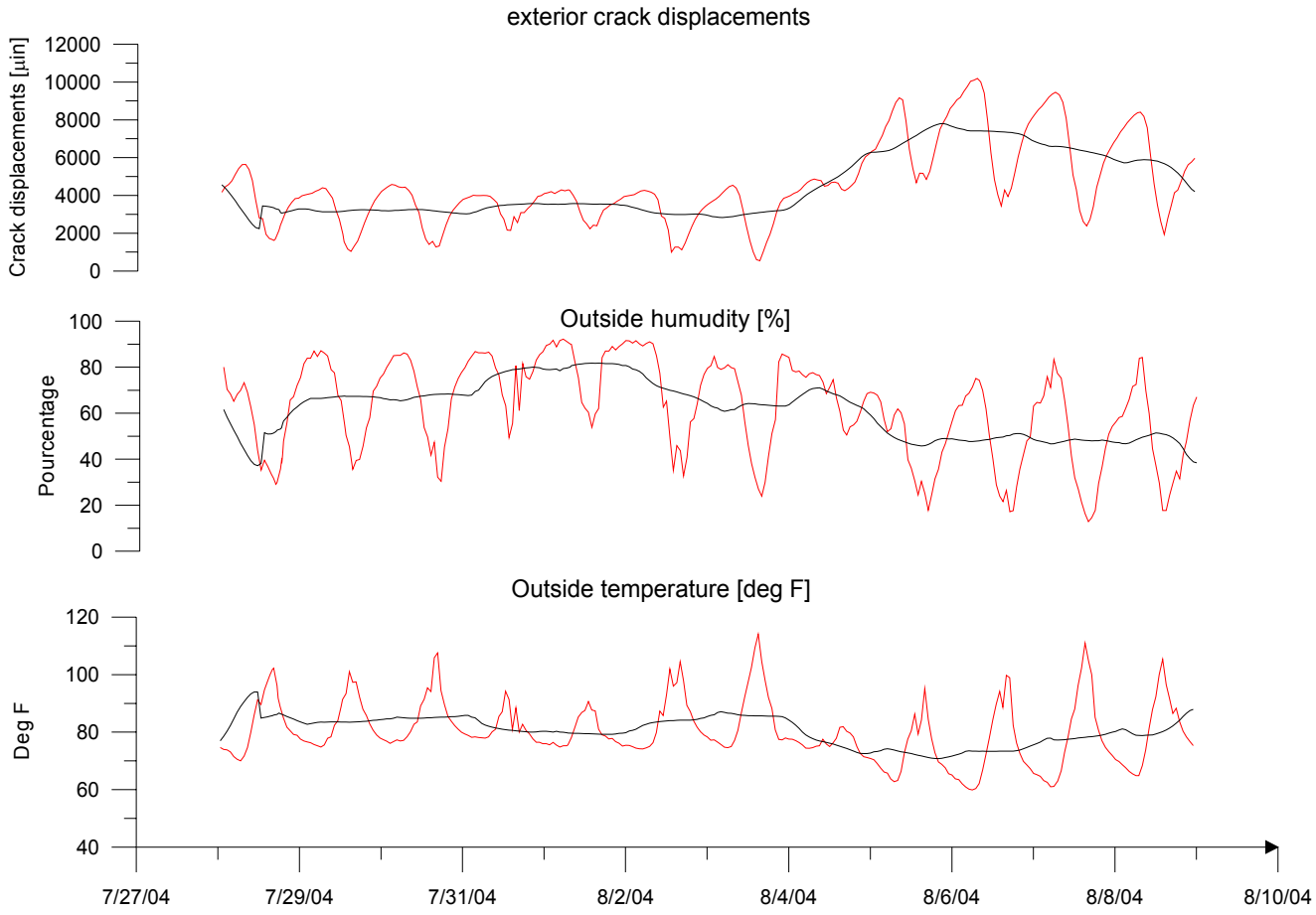

Figure 3-2: Long-term crack response and weather indicators.

Long Term triggering and Crack Response to Environmental Effects

Figures 3-3, 4 and 5 compare long-term response of cracks 1, 2 and 3 respectively, with long-term weather indicators. Temperature, Humidity and crack displacement are plotted on the same time scale. Crack displacement, humidity and temperature were measured hourly between the 19th of July 2004 and the 7th of October 2004. Figure 3-6 compares the long-term response of the three cracks where the differences described above are not easily observable. Null sensor response is also added (green) to demonstrate its insignificance. The large daily changes in the outside temperature and humidity are characteristic of an outdoor climate where the changes occur in a regular daily (temperature induced) pattern as well as a response to the passage of the weather fronts that occur on a quasi weekly cycle.

Outdoor weather phenomena correlate well with large, sharp daily changes in displacement of exterior crack 1. On the other hand, indoor crack 3 and crack 2 respond to longer-term effects. Figure 3-7 shows how crack 3 displacement correlate well with changes of inside humidity. crack 2 response is unusually large. In fact so large that it went out of the typical crack range. crack 2 is unusual in that is occurs between two separate pieces of wood molding, which respond greatly to changes in humidity. In addition crack 2 is very sensitive to human occupation as will be discussed next.

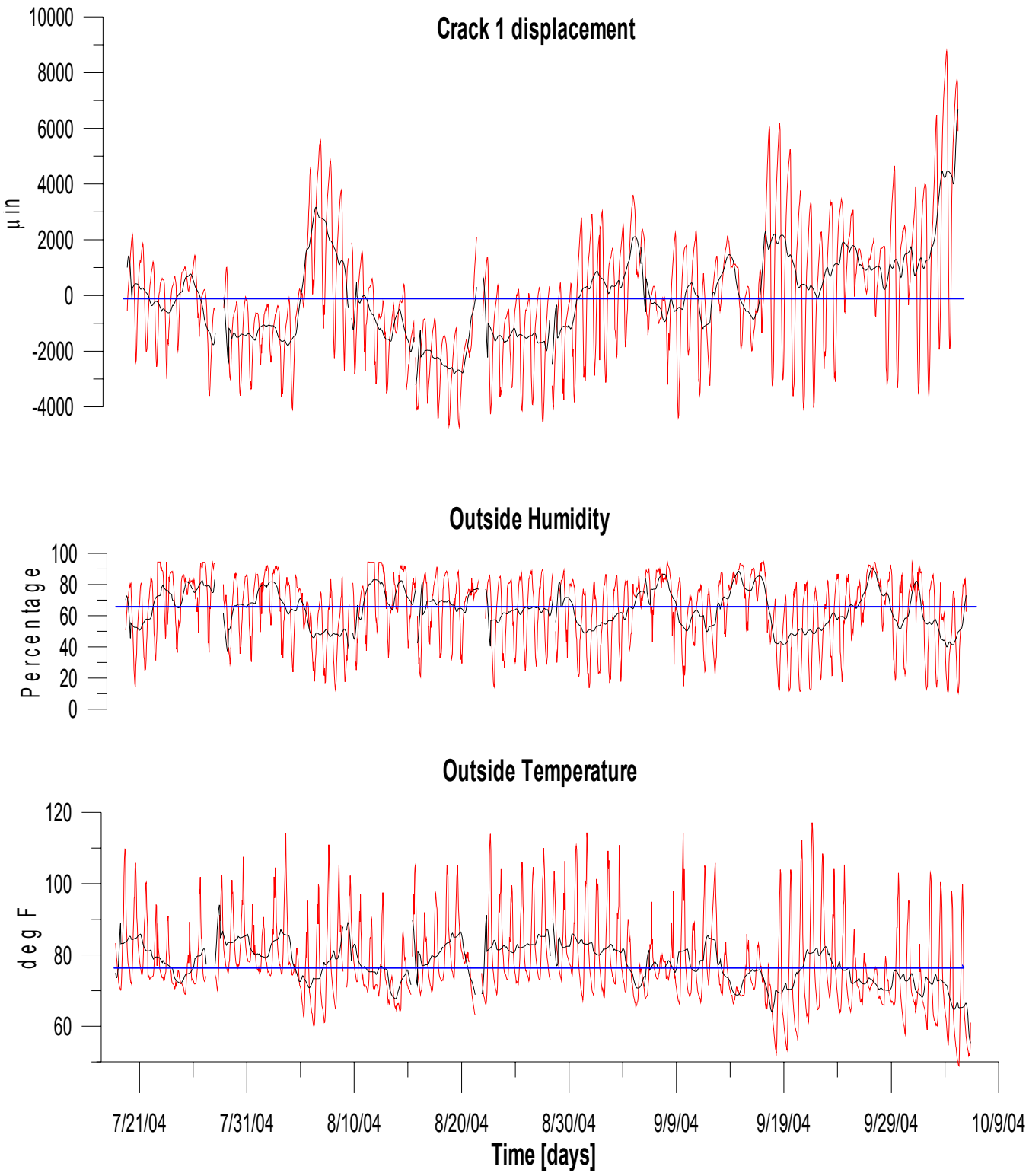

Figure 3-3: Long-term internal crack 1 displacement, outside temperature and humidity.

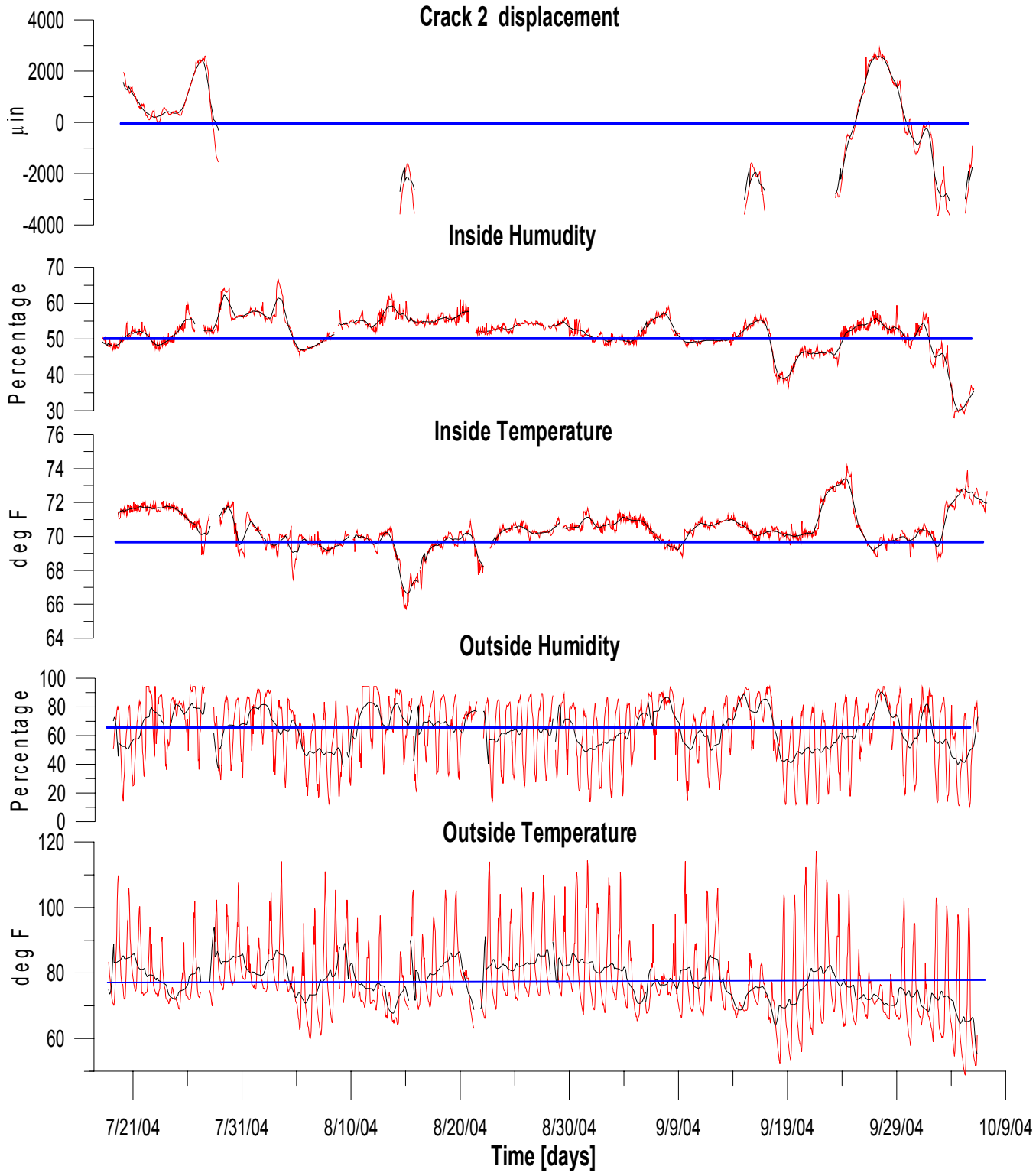

Figure 3-4: Long-term external crack 2 displacement, outside and inside temperature and humidity.

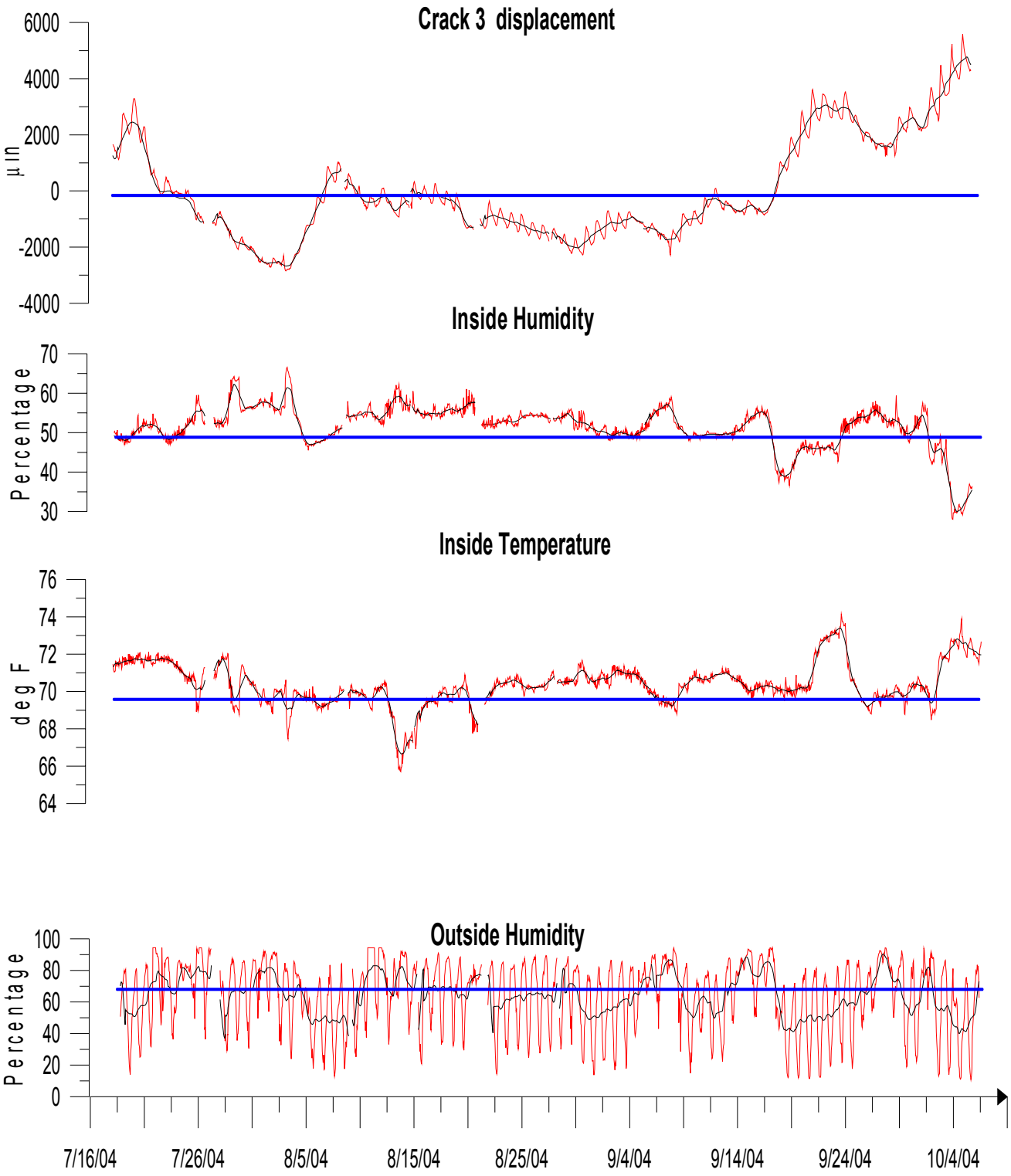

Figure 3-5: Long-term external crack 3 displacement, outside temperature and humidity and outside humidity.

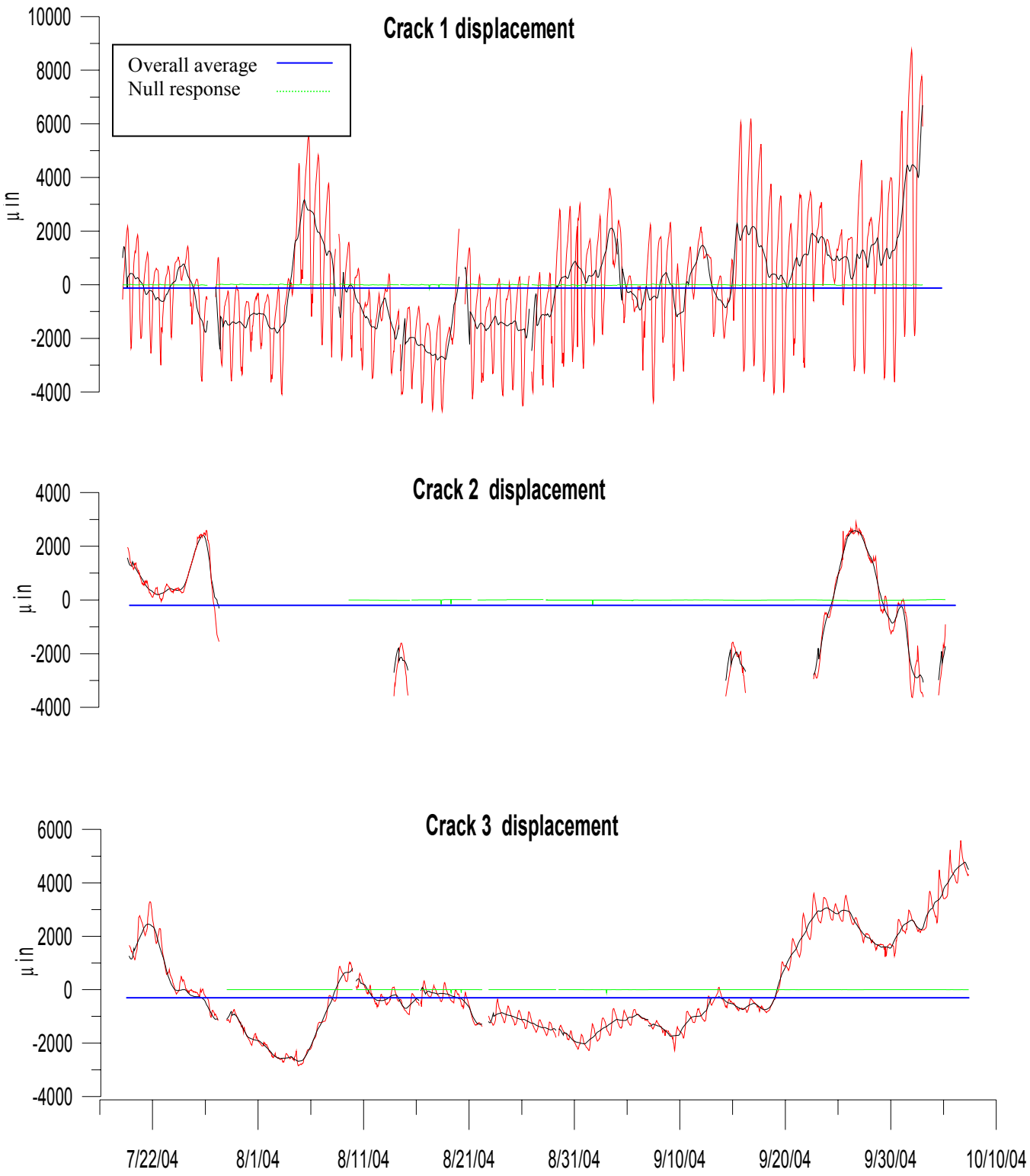

Figure 3-6: Comparison of the long-term response of all three cracks and adjacent null responses.

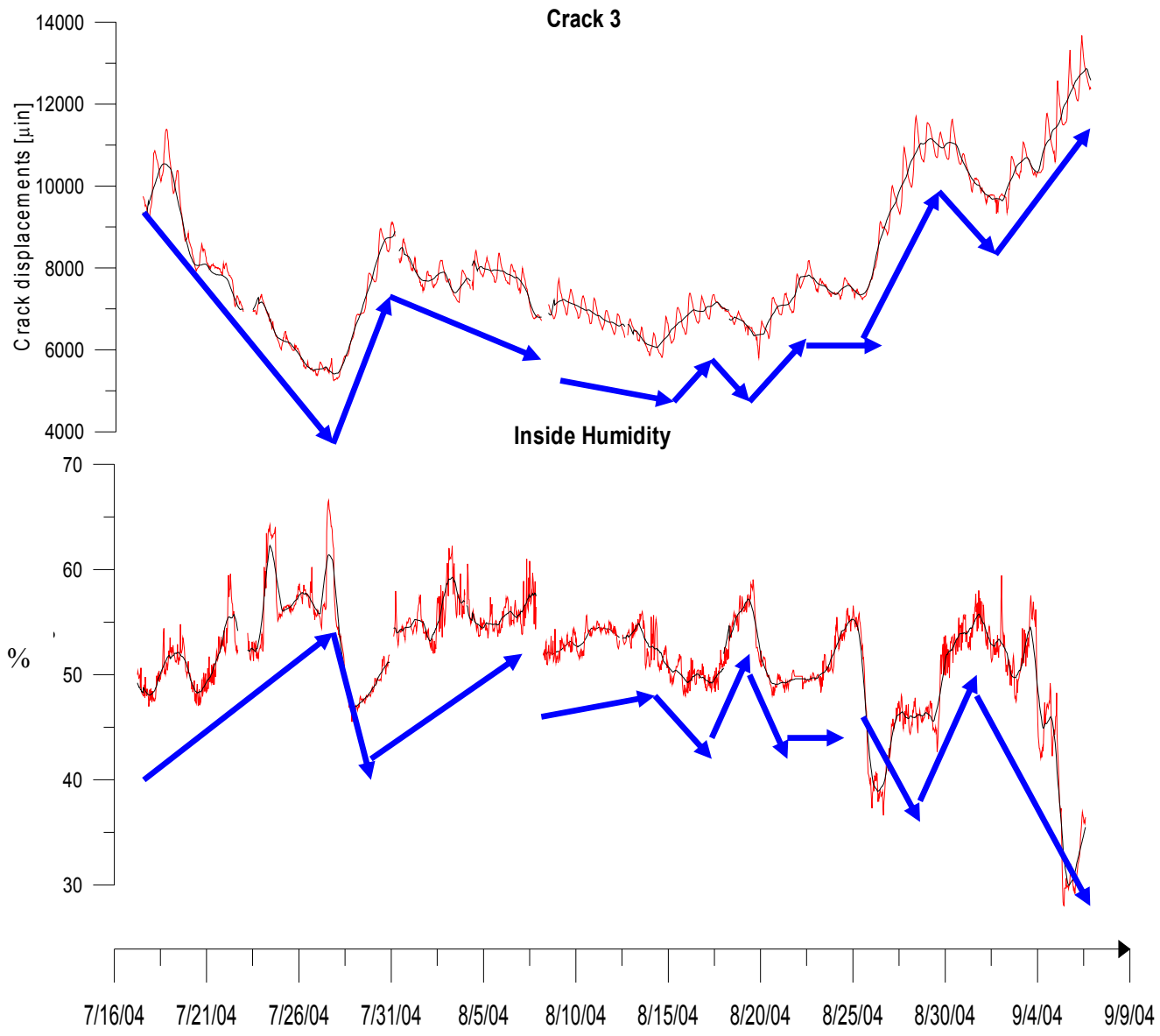

Figure 3-7: Annotated comparison of the response of crack 3 showing correlation with the long-term change in inside humidity.

Crack sensor 1- External stucco crack	Exterior Temperature Change (Deg F)	Exterior Humidity Change (%)	Crack Displacement (μin)	Crack Displacement (μm)
Frontal Effect				
Average deviation of 24-hr average from overall average	4.6	9.7	1141.7	29.0
Maximun deviation of 24-hr average from overall average	16.3	27.3	4480.3	113.8
Daily Effect				
Average deviation of field measurement from 24-hr average	8.0	15.1	1304.6	33.1
Maximun deviation of field measurement from 24-hr average	36.6	47.7	6324.6	160.6
Weather Effect				
Average deviation of field measurement from overall average	8.7	17.9	1544.0	39.2
Maximun deviation of field measurement from overall average	39.5	53.8	8762.9	222.6
Construction effect				
Maximum ground motion (PPV= 0.072 ips backhoe)	-	-	155.5	4.0
Maximum ground motion (PPV= 0.065 ips jackhammer)	-	-	101.6	2.6

Crack sensor 2- Floor molding joint	Interior Temperature Change (Deg F)	Interior Humidity Change (%)	Crack Displacement (μin)	Crack Displacement (μm)
Frontal Effect				
Average deviation of 24-hr average from overall average	0.8	3.7	1444.1	36.7
Maximun deviation of 24-hr average from overall average	3.7	21.6	2836.2	72.0
Daily Effect				
Average deviation of field measurement from 24-hr average	0.2	0.9	255.5	6.5
Maximun deviation of field measurement from 24-hr average	1.6	6.7	1293.3	32.9
Weather Effect				
Average deviation of field measurement from overall average	0.8	3.9	1515.7	38.5
Maximun deviation of field measurement from overall average	4.7	23.6	3377.6	85.8
Dial gauge between the 6/18/04 and the 7/28/04			11500.0	287.0
Construction effect				
Maximum ground motion (PPV= 0.208 ips backhoe)	-	-	53.5	1.4
Maximum ground motion (PPV= 0.164 ips jackhammer)	-	-	20.5	0.5

Crack sensor 3- Wall crack above door jamb	Interior Temperature Change (Deg F)	Interior Humidity Change (%)	Crack Displacement (μin)	Crack Displacement (μm)
Frontal Effect				
Average deviation of 24-hr average from overall average	0.8	3.7	1414.0	35.9
Maximun deviation of 24-hr average from overall average	3.7	21.6	4789.9	121.7
Daily Effect				
Average deviation of field measurement from 24-hr average	0.2	0.9	182.2	4.6
Maximun deviation of field measurement from 24-hr average	1.6	6.7	1093.0	27.8
Weather Effect				
Average deviation of field measurement from overall average	0.8	3.9	1439.1	36.6
Maximun deviation of field measurement from overall average	4.7	23.6	5583.2	141.8
Construction effect				
Maximum ground motion (PPV= 0.071 ips backhoe)	-	-	282.7	7.2
Maximum ground motion (PPV= 0.094 ips jackhammer)	-	-	29.5	0.8

Table 3-1: Tabulation of the maximum and average weather effects (maximum Frontal, Daily and Weather) as well as construction effects.

The effects of the various changes in weather on crack displacement are compared to the vibration induced crack displacement in Table 3-1. The manner in which these effects were determined is explained in conjunction with Figure 3-1 b. Both an average and a maximum value relative to the overall averaging during the three months of observation are tabulated. Measurements of the construction vibration effects are described in the following chapter. The weather-induced effects on external crack 1 were significantly larger than for internal crack 2 and 3. Both the interior floor molding crack 2 and wall crack 3 will be the object of separate special studies of occupant induced response. This disparity in magnitude between internal and external makes sense, as the inside temperature and humidity are controlled and are not subjected to direct sunlight.

In addition the outside humidity, rainfall was also tracked and compared in Figure 3-8 with the outside humidity. Apparently the climate was humid enough that rainfall alone was not a major influence in humidity.

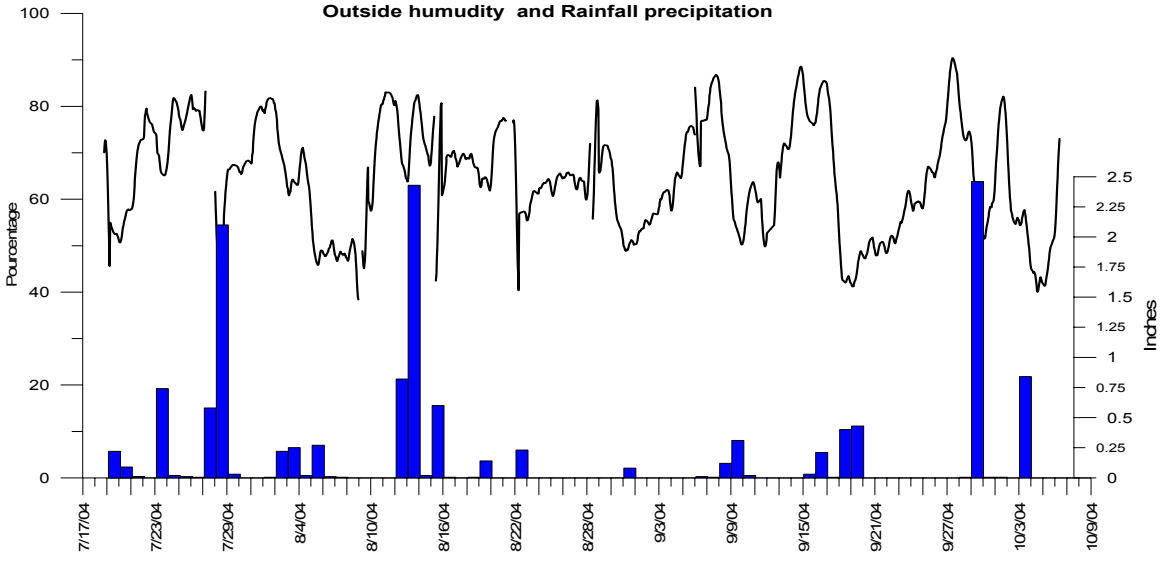

Figure 3-8: Comparison of rainfall with outside humidity.

Between visits on 18 June and 28 July, the crack 2's displacement was so large that it went out of range. As shown in Figure 3-9 the dial gauge across this crack (installed by another group) showed a displacement of some 0.0115 in (287 μm), which explains why crack 2 sensor exceeded its 0.005 inch range. Among the possible causes of the unusually large-displacements was the large moisture driven response of wood.

a) b)

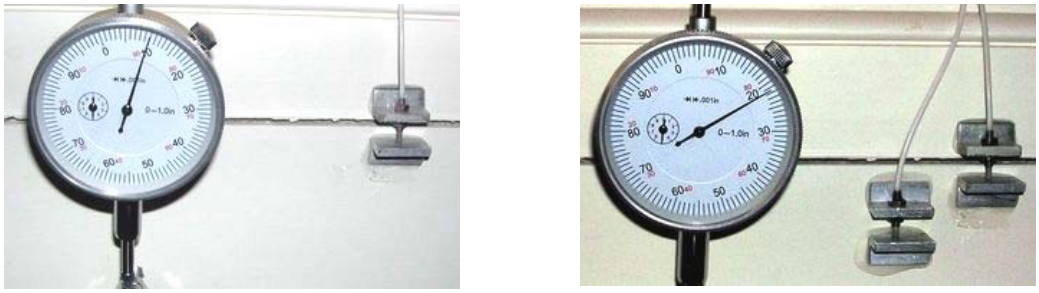

Figure 3-9: Large displacement of joint between two pieces of molding verified as dial gauge, a) the 6/18/04 and b) the 7/28/04.

Occupant Activity Response

Manual triggering was employed by ITI staff while on site to collect interior crack 2 and 3 responses to occupant activity. Response of the molding joint crack (crack 2) was collected as a person walked back and forth twice and then sat on a chair near the crack. The sequence lasted fifty seconds, during which one point was collected every millisecond in order to accurately correlate crack response with respect to time of activity. Response of the wall crack (crack 3) was collected as a person walked through the doorway, leaned on the door's jamb or slammed the door. Data were collected every millisecond for crack 3 as well.

Figure 3-10 compares response of the molding crack joint to the activity shown in the thumbnail photographs. As the person walks by the floor adjacent to crack 2, it expands and then contracts. The first round trip produces two such spikes. During the second "round trip" the person passed closer to the woodwork crack than at first. The crack again responded instantaneously but with larger displacements. When the person sat on the chair for 4 seconds the crack again expanded straight away almost 18 μm, and just as it started 4 seconds before, the expansion ceased quickly after the person stood up from the chair.

Crack 2's behavior has little in common with the other two. As will be shown later ground motions produced a displacement of only 1.36 μm, whereas it expanded some 22.65 μm during the special occupant study. The molding joint response may have resulted from different attachment to the wall and floor. The upper member may be attached to the wall whereas the lower member maybe attached to the floor. Both parts

may respond to both changes in the weather and occupant activity independently from each other, which explain why the crack responded so highly much to human interaction.

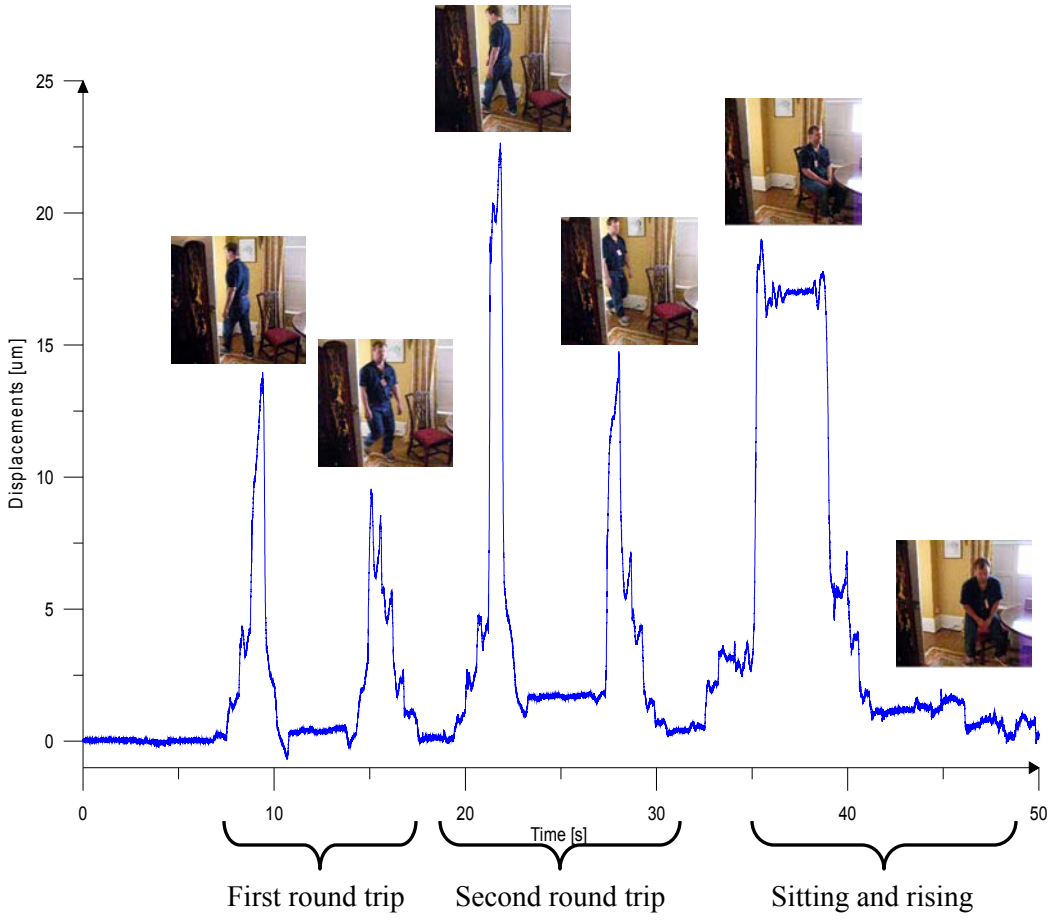

Figure 3-10: Time sequence of crack 2 displacement and occupant activity.

Figure 3-11 shows the two minute special study performed on crack 3. Crack 3 displacement is plotted with respect to time as in Figure 3-10. Rooms and door frame containing crack 3 are labeled on the plan view insert. Crack 3 responded instantaneously to human excitation by expanding and contracting, as did crack 2. Albeit the first

opening and closing of the bedroom door created relatively small displacement (2 µm or 80 µin), slamming the bathroom door induced the largest crack 3 displacement of 15 µm (600 µin). As will be discussed in Chapter 4, the responses to leaning are important because the same pattern was observed during a period of interior work, which occurred during jackhammer excitation.

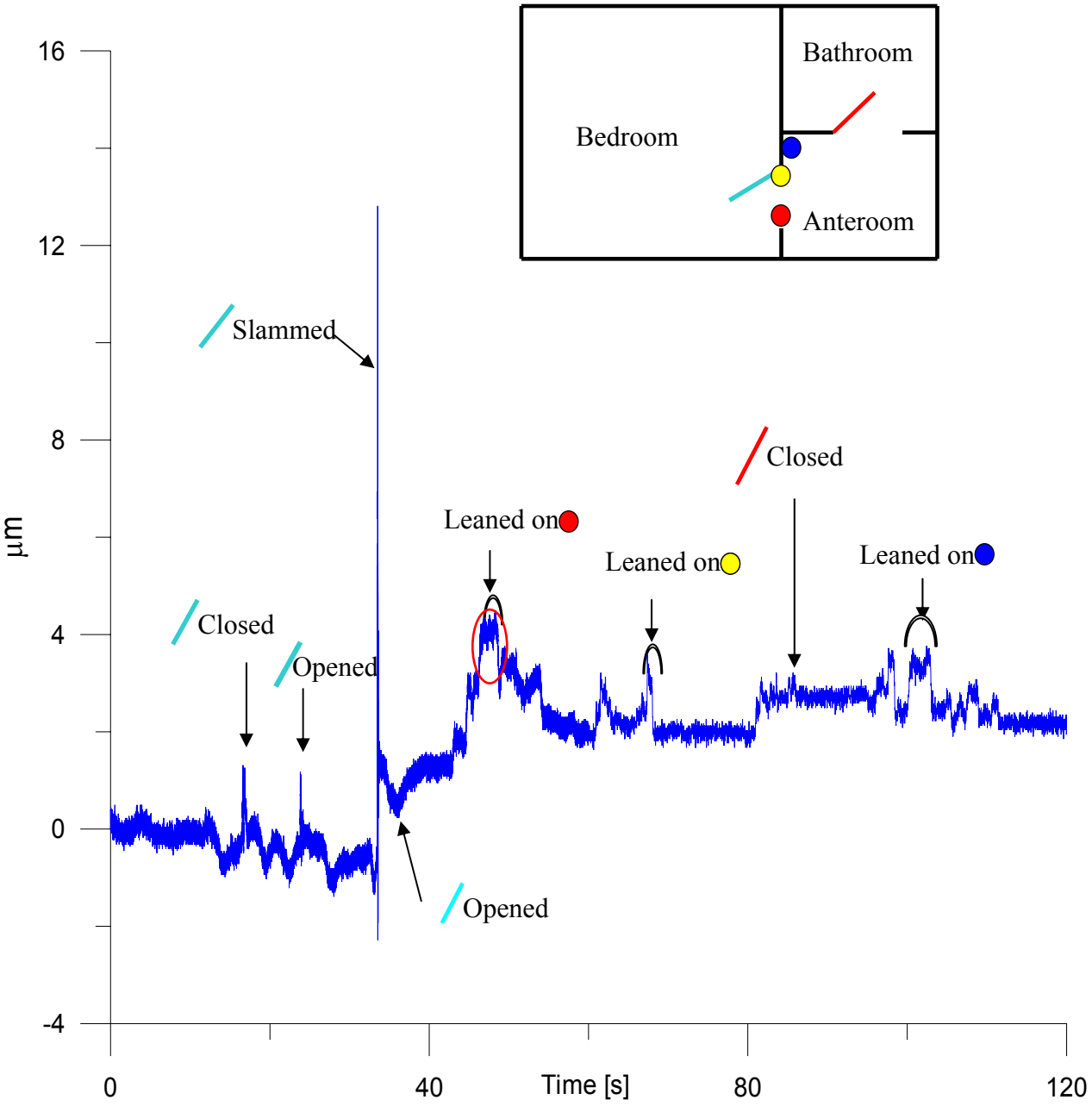

Figure 3-11: Time sequence of crack 3 displacement and occupant activity.

CHAPTER 4

Construction Vibration Response

Introduction

The highly variable construction vibration environment in front of the house required a flexible triggering scheme to collect responses from both continuous sources as well as isolated transient events. Indeed, possibly hundreds to thousands of daily events would have to be measured, which differs from blast vibrations that typically occur only a few times a day or a week, last for a few seconds, and involve relatively standard ground motions. Vibratory crack and ground motion data were collected during nearly 3 months, between the 19th of July 2004 and the 7th of October 2004.

Five triggering mechanisms

Five different triggering mechanisms were employed to autonomously record the vibrations produced by construction. As there was no possibility for daily on-site inspection, it was important to be able to autonomously measure the varied and often continuous activity in the vicinity of the structure. Roadway reconstruction involves different types of heavy machines or vibratory sources such as vibratory rollers, jackhammers, backhoes and pavement breakers. Hence the triggering system must be sophisticated enough to record significant responses from machines that produce a widely varying vibration signature.

The first triggering mechanism enables long-term data collection. In this specific configuration, the system is triggered for 1/1000th of a second every hour for the duration of the test. Only one point is recorded per hour. This single point will define the crack response to long-term or environmental effects. Kaman crack sensors as well as weather data were recorded in this manner. These long-term data were presented in the preceding chapter.

The second triggering mechanism is the so called ground motion environment. In this mode samples are collected at a thousand hertz continuously during one minute, and the highest value among these 60,000 points is retained. Then another one minute recording period begins and so on. These peaks were recorded for each of the three axes of the geophone. This triggering mode was developed to capture vibratory roller data. While rollers were not employed in this phase, this trigger mode was useful to define general jackhammer activity.

A third triggering mode enables the collection of time histories of ground velocity and crack displacement for single, transient vibratory events. Collection typically begins whenever any of the three geophone components exceeds the preset trigger level of 0.04 ips. The system then collects data at 1000 Hz for 2 seconds after the triggering point and for the preceding second. In other words, it collects 3001 points during 3 seconds (and one millisecond). Data preceding the trigger are collected to ensure initial, but lower intensely data are collected.

The forth triggering mechanism involves the collection of significant events that occur over a long period of time. Pushing the trigger switch manually allows continuous recording at a 1000 Hz sample rate until the button is pushed again. Since there were no on-site personnel to manually activate the system, this mechanism was only used twice when ITI staff members were on site. Data obtained from the manual triggering was described in the section on occupant activity.

The fifth triggering mechanism involves the collection of responses of the three cracks when one of their displacements exceeds a preset value. This mechanism is still under development as it requires a trigger based on a dynamic from the average of the previous crack displacements. Unlike a geophone that outputs zero voltage at rest, a sensor across a crack expanding and contracting from weather effects will output a variable voltage.

Ground Motion environment

The ground motion environment as defined by the second triggering mechanism has been plotted in Figure 4-1 for the full monitoring period. Although ground motions in the longitudinal, transverse and vertical directions are collected for the singular trigger events, only the ten largest vertical peak particle velocities (PPV) for each day are presented. Most of the PPV fall below 3 mm/s (0.1 in/s) with only a few larger events. Time histories of these larger events were also recorded through the third triggering mechanism.

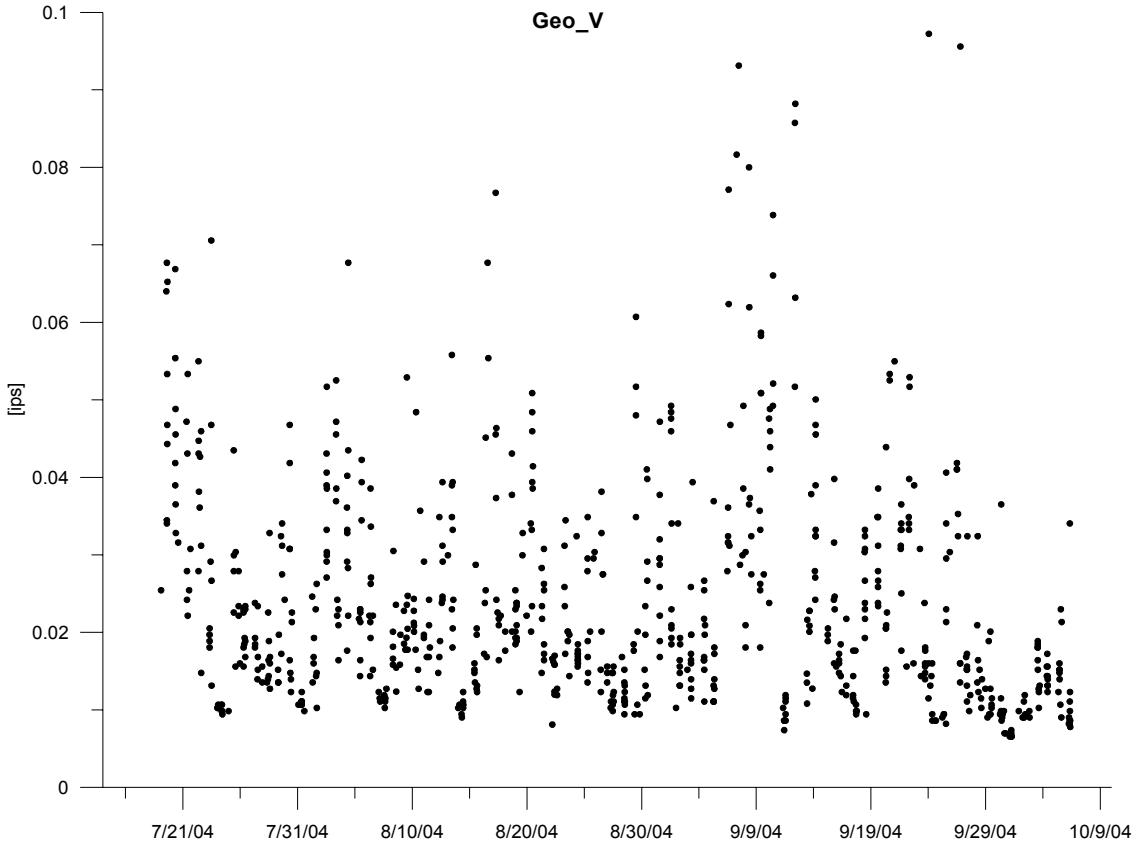

Figure 4-1: Ground Motion Environment showing periods of elevated activity.

The introduction of the chapter noted the need of an elaborate system able to properly capture the full extent of ground structural response. Among the many events recorded during construction were a large number of spurious “noise” events. All spurious events had the same pattern as that shown in Figure 4-2. Their special time history signature allows them to be segregated from triggered construction vibration events.

Noise events last for only one or two samples (if it has a frequency larger than 500 Hz) and there is no crack response about the noise level. Figure 3-2 compares the three second long time history of the displacements of the three cracks (top) and the time correlated longitudinal, transversal and vertical ground motions. These noise spikes could not be caused by human activity such as walking as they would be of lower frequency and show multiple peaks over a three second interval of time.

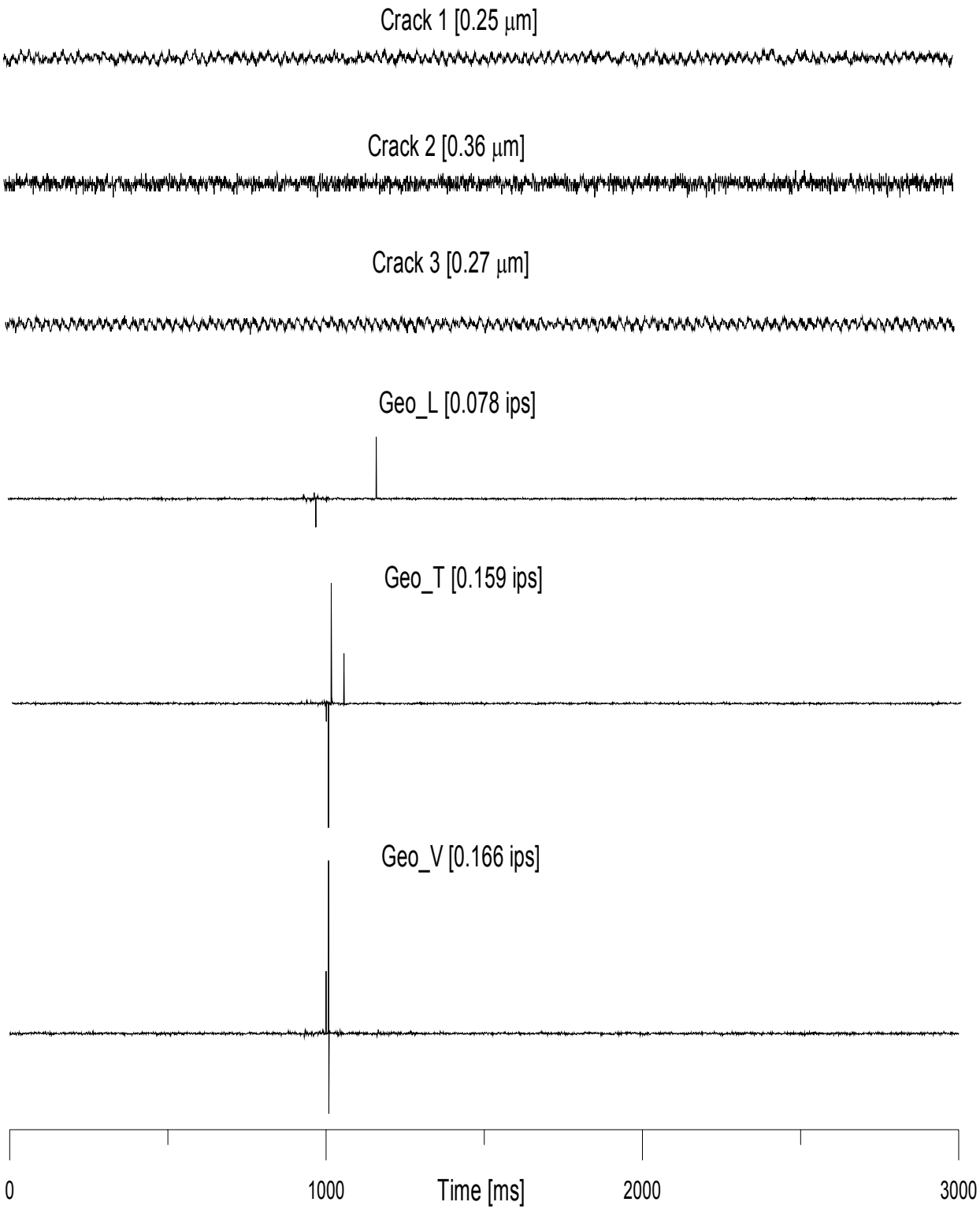

Figure 4-2: Electrical noise event showing spike signature and no crack response.

Backhoe Activity

Tow events produced by backhoe trenching describe the range of excitation and crack response. These two time histories of excitation ground motion and associated crack responses are shown in Figure 4-3. They occurred at 7:49 AM on July 27th (event 3) and at 9.52 AM on July 22nd (event 9), 2004. The trenching line shown in Figure 2-2 was oriented parallel to the façade and was located within several meters of the house. Figure 4-3 compares excitation and response for both events on the same graph. To eliminate the non-relevant noise in the comparison of events 3 and 9 only 1.6 seconds of crack response was plotted. During the first event the excitation induced a maximum crack 1 displacement of 3.95 μm, and one of the largest crack 3 displacements with 5.90 μm.

These two events were selected from 27 events summarized in Table 4-1 that produced the largest crack responses. They are significant because similar peak particle velocities produced different crack displacements. Although similar peak particle velocities were recorded for both events 3 and 9, vibratory responses for event 3 were respectively 3.95 μm (158 μin) and 5.90 μm (236 μin) for crack 1 and 3, but only 0.49 μm (20 μin) and 0.81 μm (32 μin) for event 9. This difference in response can be explained by studying the frequency content of the excitation ground motions by employing the Frequency Fourier Transform (FFT) method (Dowding, 1996). Figure 4-4 is an FFT spectrum that shows a dominant frequency of 12.5 Hz and 45 Hz respectively for event 3 and 9, for the longitudinal ground motion.

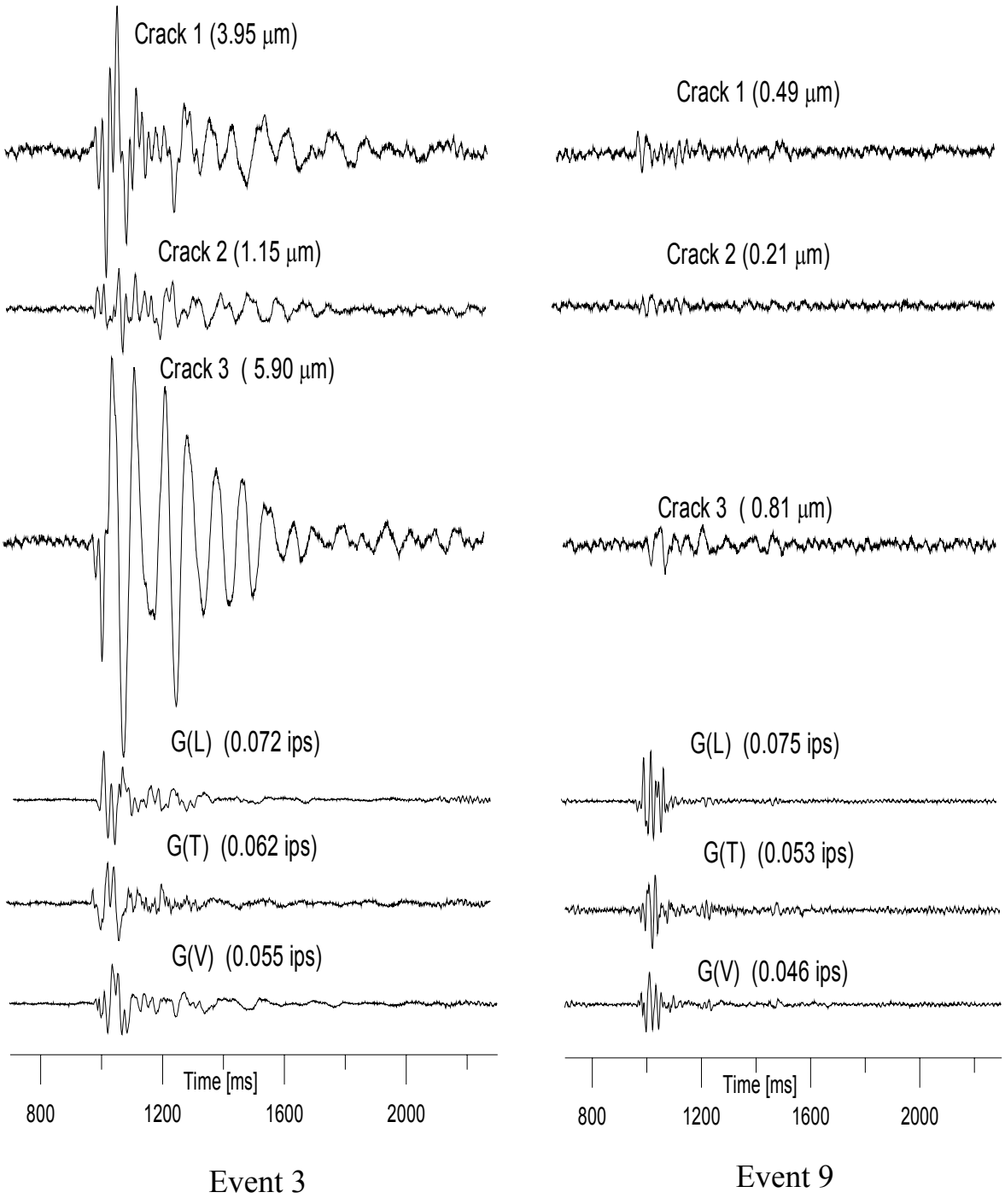

Figure 4-3: Comparison of excitation ground motion (lower 3 time histories) and crack response (upper 3 time histories) to demonstrate the importance of excitation frequency.

event date	event #	L [ips]	T [ips]	V [ips]	crack 1 [μm]	ground calculated displacements	crack 2 [μm]	crack 3 [μm]	Frequency [Hz]
									L
7/20/04 14:30	1	0.023	0.077	0.041	0.37		0.19	0.56	
7/20/04 14:30	2	0.036	0.071	0.031	0.28		0.27	0.77	
7/21/04 7:49	3	0.072	0.062	0.055	3.95	0.0058	1.15	5.90	12.5
7/21/04 7:49	4	0.046	0.057	0.071	3.11		1.01	7.18	
7/21/04 7:50	5	0.053	0.067	0.052	2.84		0.87	5.50	
7/21/04 7:50	6	0.033	0.068	0.047	2.08		0.66	5.90	
7/21/04 7:50	7	0.039	0.059	0.059	2.15		0.80	7.17	
7/22/04 7:14	8	0.046	0.119	0.057	1.20		0.24	0.86	
7/22/04 9:52	9	0.075	0.053	0.046	0.49	0.0018	0.21	0.81	41
7/22/04 12:39	10	0.022	0.105	0.044	0.54		0.19	0.57	
7/24/04 11:12	11	0.025	0.075	0.056	1.87		0.75	3.17	
7/24/04 11:12	12	0.080	0.037	0.058	2.73		1.04	2.77	
7/24/04 11:12	13	0.119	0.039	0.063	3.28		1.08	3.02	
7/24/04 11:12	14	0.150	0.035	0.075	3.33		1.26	2.42	
7/24/04 11:12	15	0.208	0.069	0.051	3.16		1.36	2.17	
7/24/04 11:12	16	0.162	0.060	0.061	2.16		1.06	2.29	
8/17/04 13:28	17	0.039	0.126	0.051	0.42		0.39	1.86	
8/17/04 13:29	18	0.065	0.110	0.053	0.40		0.46	1.72	
8/17/04 13:29	19	0.055	0.071	0.035	0.35		0.38	1.67	
8/17/04 13:29	20	0.067	0.110	0.071	0.42		0.39	1.56	
8/17/04 13:39	21	0.060	0.064	0.046	0.68		0.38	1.61	
9/13/2004 8:49	22	0.065	0.052	0.058	2.59		0.38	0.47	
9/13/2004 8:49	23	0.058	0.094	0.030	1.82		0.44	1.60	
9/13/2004 8:49	24	0.056	0.117	0.032	1.33		0.47	1.89	
9/13/2004 8:49	25	0.068	0.112	0.036	1.60		0.45	0.95	
9/13/2004 8:49	26	0.064	0.164	0.052	2.16		0.52	0.52	
9/13/2004 8:49	27	0.060	0.097	0.083	2.06		0.43	0.44	

Table 4-1: Most vibratory energetic events. Events 1 to 21 produced by backhoe and 22 to 27 produced by jackhammer.

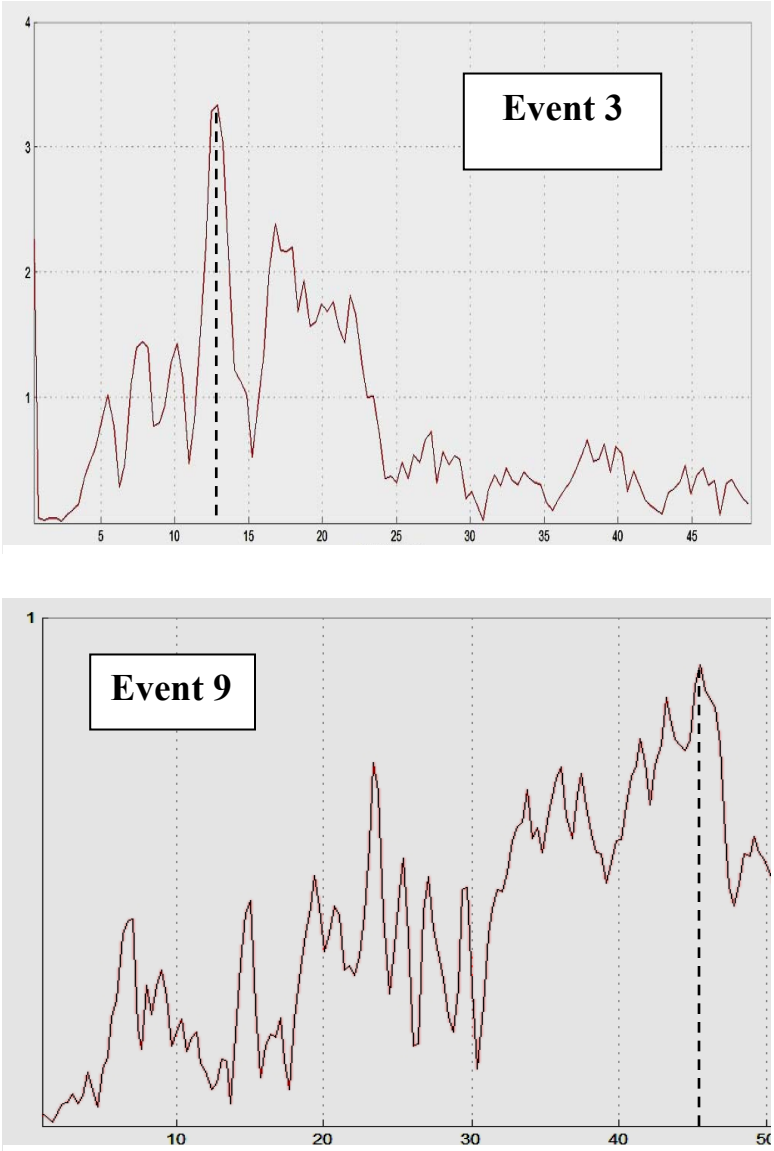

Figure 4-4: Fourier frequency spectrum of excitation ground motion for backhoe events 3 and 9.

Excitation frequency is important as structures respond more when the excitation frequency is near that of the natural frequency of the structure or its components. Natural frequencies of the superstructure are inversely proportional to the height of the structure (ie 10 Hz for one storey and 5 Hz for two storey structures). Natural frequencies of walls and floors tend to fall in the 10 to 20 Hz range. Thus ground motions whose dominant frequency is near 12 Hz (event 3) would be expected to cause greater structural response than those whose dominant frequency is more than 40 Hz (event 9).

Figures 4-5. 6 and 7 are time histories of three jackhammer events (22, 23 and 24 in Table 4-1, at 9:49 am on the 13th of September 2004) and the associated crack 1, 2 and 3 responses. The three were selected from the 99 events collected on that morning. Event 22, typical of many of the events produced the maximum response 2.58 μm (103 μin) for crack 1. Crack 1 consistently had the maximum response. Crack's 3 response was much lower (< 0.5 μm) after the occupant induced response was subtracted. Crack 2 response was never greater than the noise level.

Crack 3 responses for events 23 and 24 both include a very low frequency arch associated with occupant activity. An "arch" occurs in the crack 3 displacement histories between seconds 5 and 6 for event 23, and between seconds 2 and 3 for event 24. Both arches are between 1.60 and 1.86 μm in magnitude. The arch in event 23 occurs during a period of quiescence, which implies a source other than vibration. Management of the house indicated that during that time workers were active in the third floor rooms containing the door jamb above which crack 3 was located. Details of this human activity were discussed in Chapter 3. For convenience, excitation crack response for backhoe events 3, 9 and jackhammer event 22 are compared in Figure 4-8 at the same scale.

Figure 4-9 compares occupant induced crack 3 responses measured during jackhammer special study with response to events 23 and 24. The lower right time history is the crack 3 response to a quick lean on the jamb of the bathroom door (red circle in Figure 3-11), and the one on the bottom left occurred during jackhammering event number 23. Both crack 3 responses are similar. In both cases crack 3 expanded from a relative zero to approximately 1.2 μm (48 μin) in 0.4 seconds, and remained at that level until contracting over the same length of time. These rise times are similar to those observed during the occupant test for crack 2. The main difference between these two responses is that the left "arch" lasts 2.7 seconds whereas the right arch last less than 1.2 seconds. This difference is probably the result of the length of contact while leaning on the door's jamb.

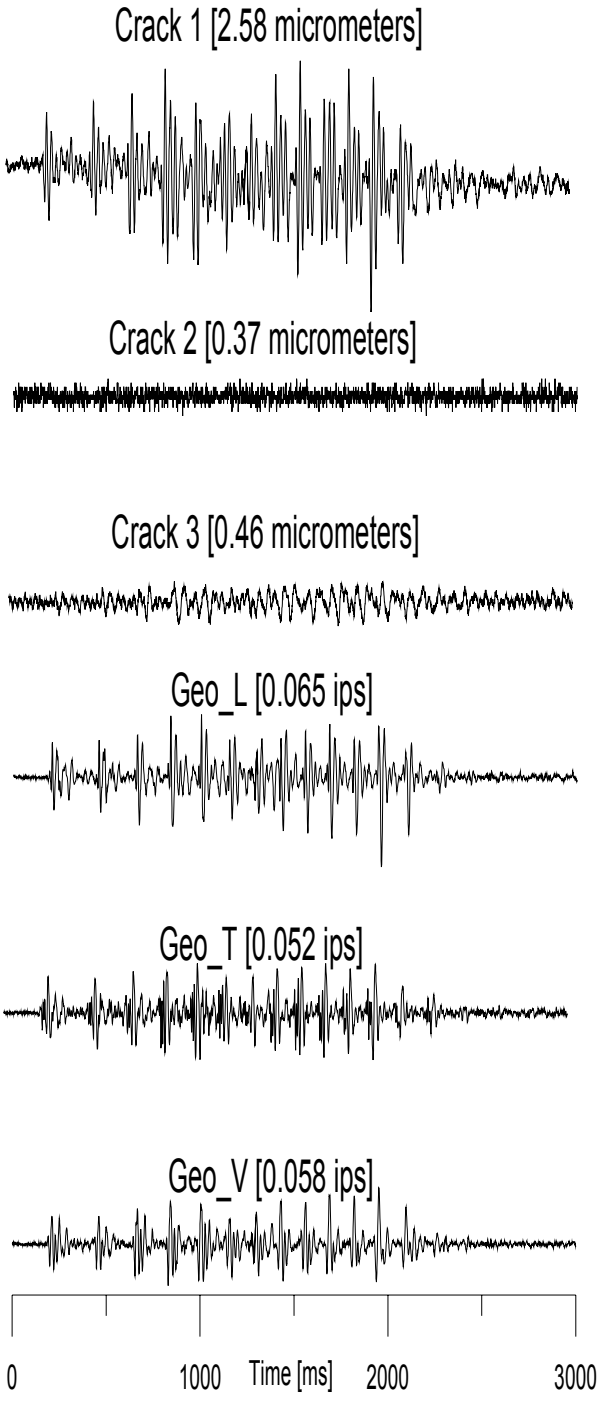

Figure 4-5: Maximum response of crack 1, which responded the most to the jackhammer excitation.

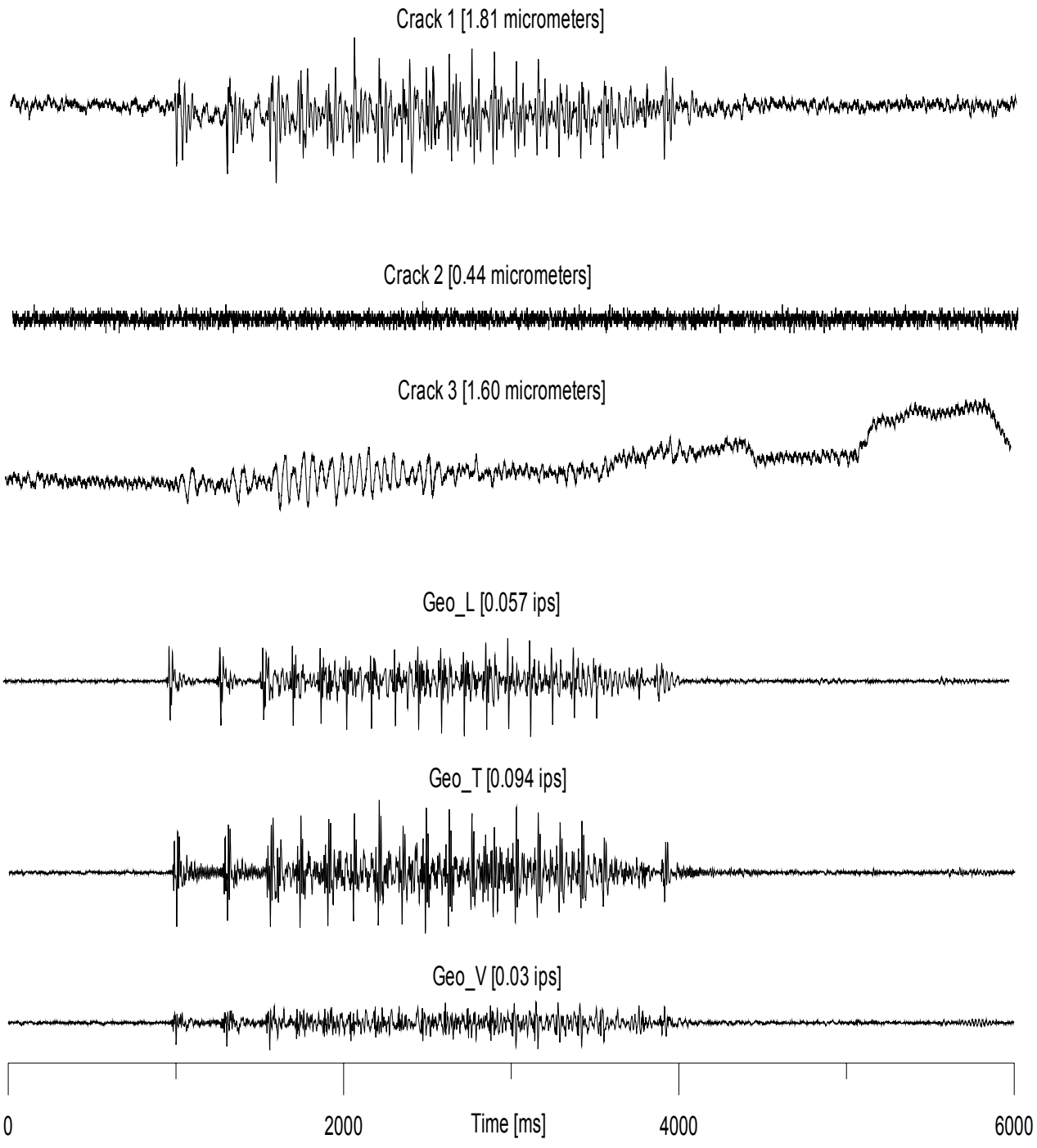

Event 23

Figure 4-6: Jackhammer event 23, showing an occupant induced response in crack 3 during a period of no vibration response.

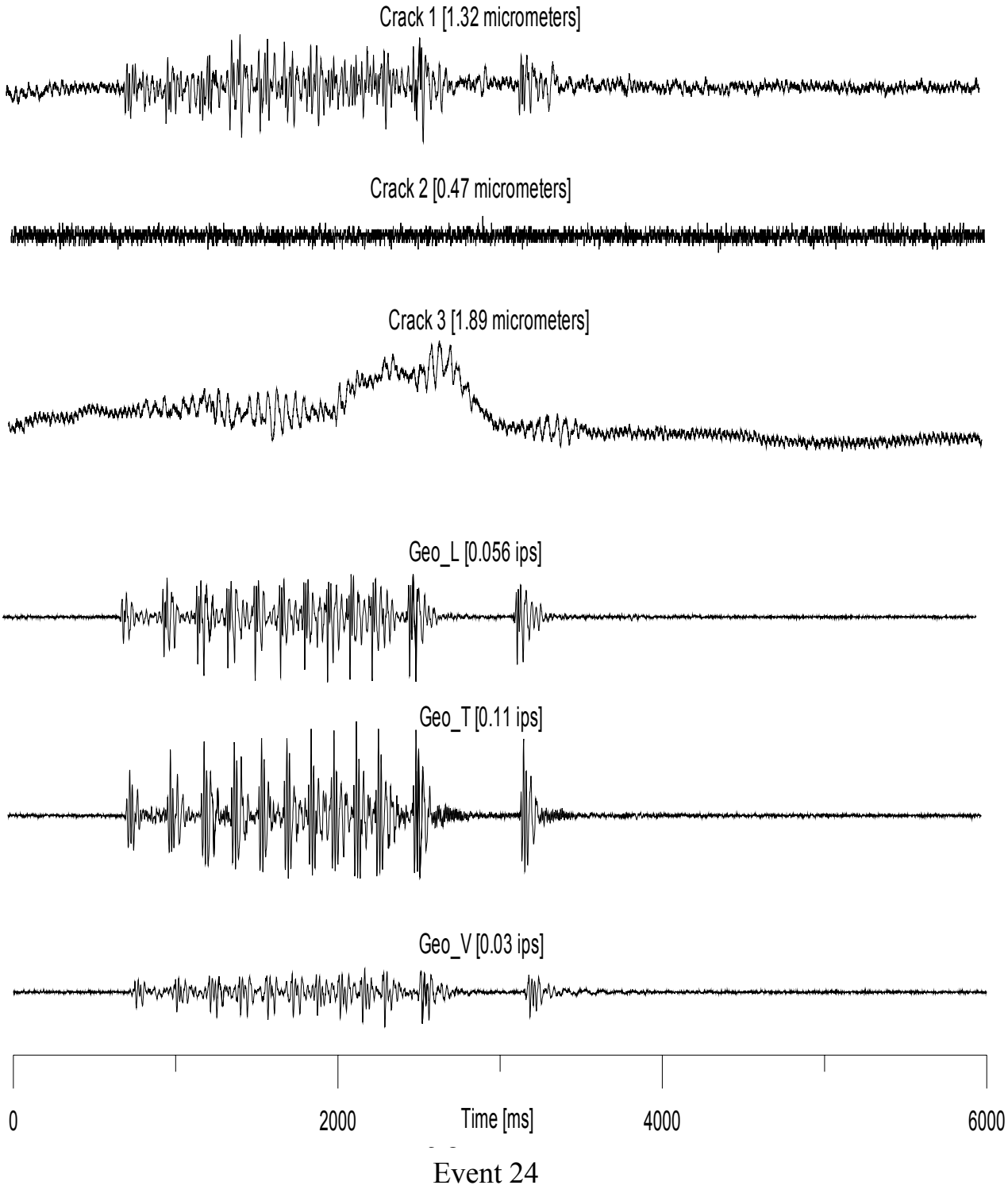

Figure 4-7: Jackhammer event 24, showing a coincidence of the occupant induced and vibration induced response of crack 3.

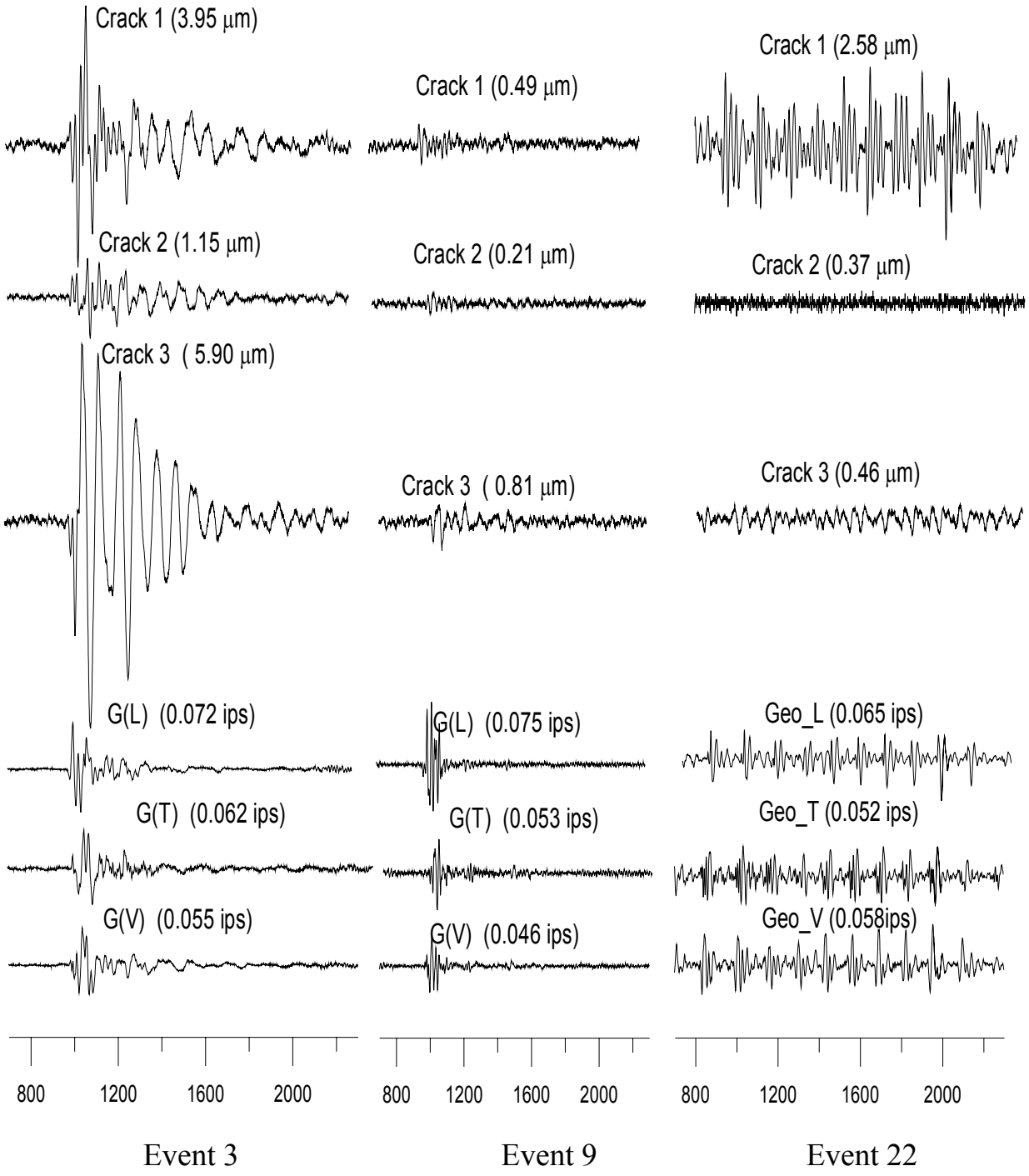

Figure 4-8: Comparison of events 3, 9 and 22.

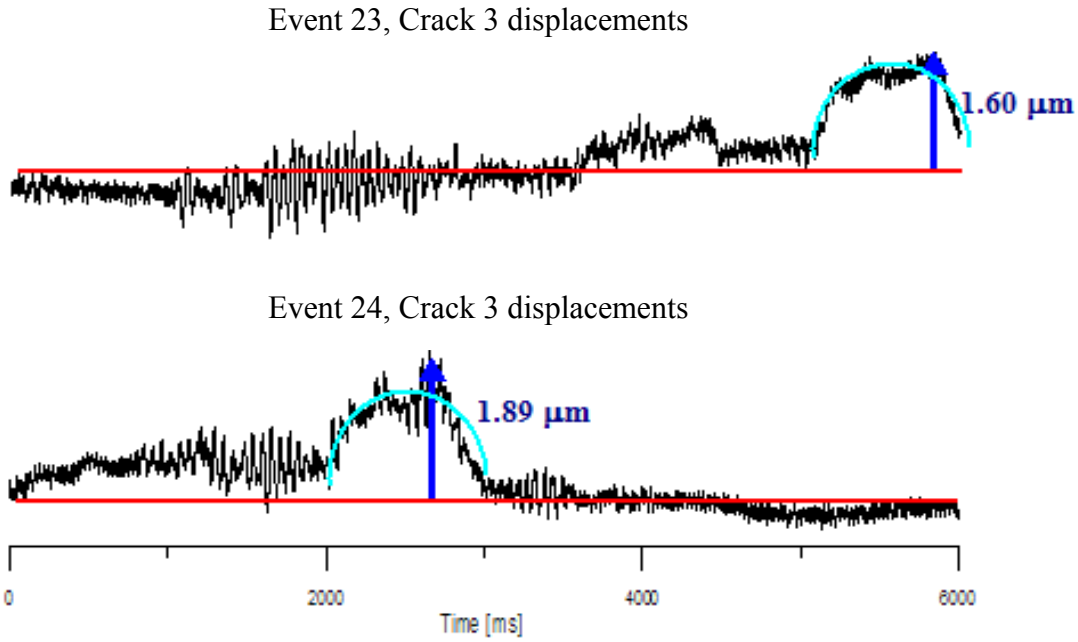

a) Simultaneous occupant induced and jackhammer excitation

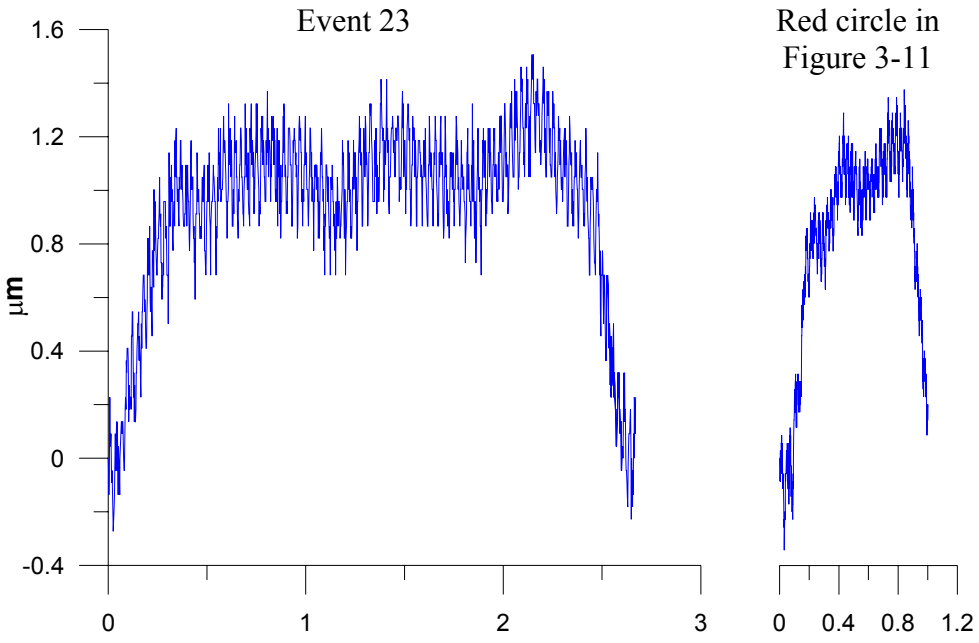

b) Comparison of occupant induced responses

Figure 4-9: Comparison of occupant induced crack displacements measured during jackhammering and special study.

Figure 4-10 compares response of crack 3 displacement during an energetic slamming of the bathroom door and the long-term cyclic weather effects. The long-term effect is plotted over a period of 8 days (in red), whereas 40 seconds surrounding the door slam are expanded in the inset in order to be seen. This expansion itself demonstrates how large and significant are the long-term cyclic weather effects. As the graph shows, in 8 days crack 3 widened some 100 μm (4000 μin) versus 15 μm (600 μin) when the door immediately below was energetically slammed. The long-term effect is then more than seven times larger. Cyclic daily changes show that the crack opened and closed some 25 μm (1000 μin) each day.

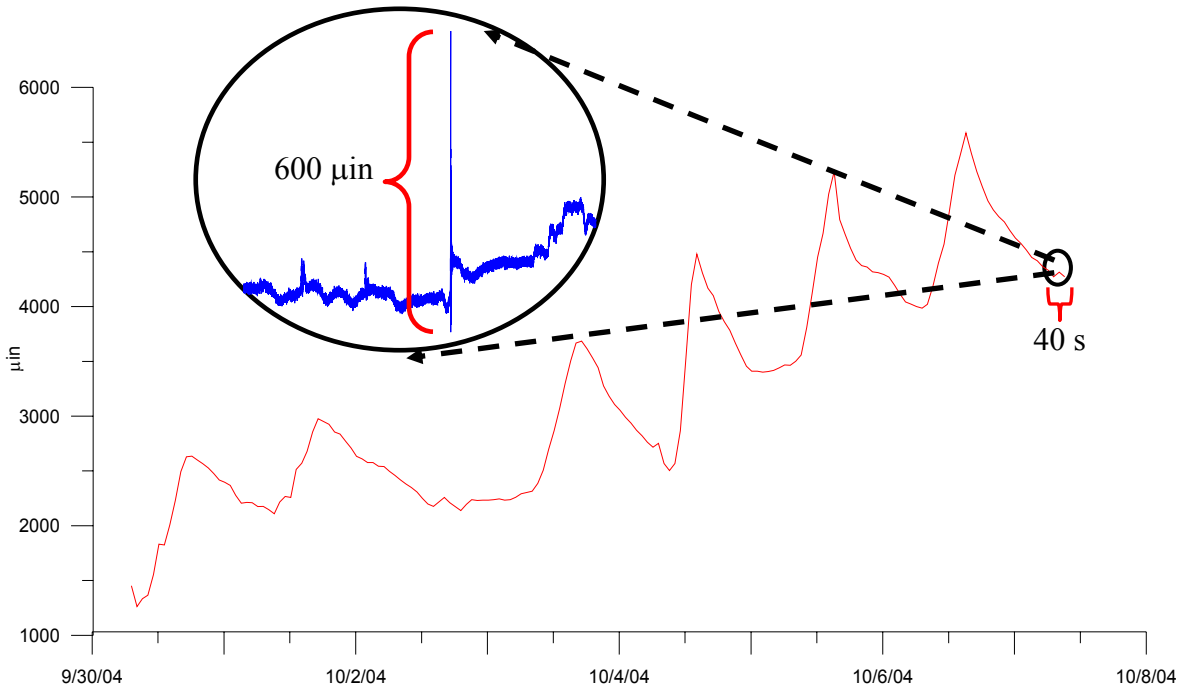

Figure 4-10: Crack 3's 24-hour average and magnified door slam event.

Figure 4-11 compares the long-term or weather with the construction vibration-induced displacement responses for the three instrumented cracks. The maxima of all three types of effects (weather, occupant and construction vibration) are compared. In all three cases the long term maximum weather effect produces the largest displacement, which is more than 10 times greater than that induced by the maximum vibration event during the adjacent construction. Daily effects dominated the response of crack 1 probably because of its direct exposure to sun on the south facing wall. On the other hand weekly or frontal effects dominate the response of the interior cracks 2 and 3. Occupant or human effects produced much greater effects than construction vibration. As discussed in the last section, simply leaning on the door jamb produces significant crack displacement.

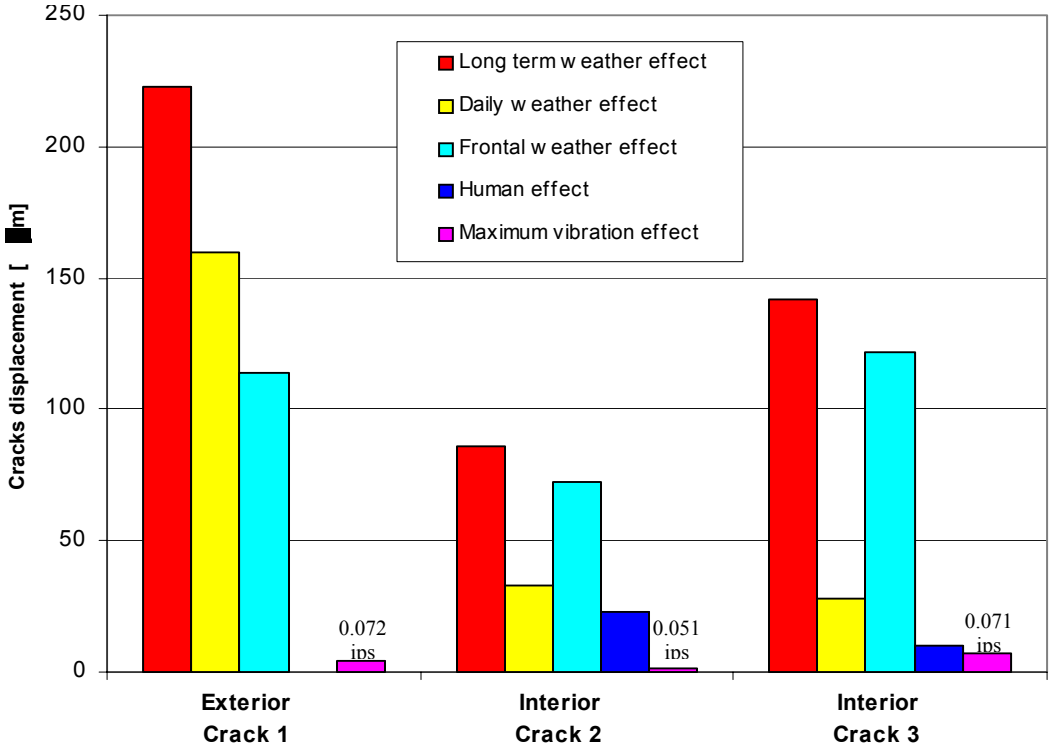

Figure 4-11: Comparison of weather, occupant and construction vibration induced displacement of all 3 cracks.

CHAPTER 5

Conclusions

This thesis summarizes micro-inch response of cracks in a historic structure to construction-induced ground motions and environmental phenomena. The structure was located in downtown Washington DC. It was instrumented and its response was studied as part of the development of an Autonomous Crack Measurement (ACM) system sponsored by the Infrastructure Technology Institute at Northwestern University through a block grant from the United States Department of Transportation. This specific demonstration project was made possible by the cooperation of the Eastern Federal Lands division of FHWA and the Department of State.

Ground motions at the Washington D.C structure were measured with a buried tri-axial geophone block customary in all previous ACM sites. Micro-inch displacements of three cracks were measured with Kaman sensors. One sensor was placed across an exterior crack in the stucco façade. One of the two instrumented interior cracks was a joint between two pieces of floor molding and the second crack was in the plaster lath wall above a door jamb. Construction adjacent to the house involved trenching for the rehabilitation of the street and replacement of underground utilities. Special precautions were undertaken to minimize vibrations adjacent to the historic structure.

The synthesis of measurements and calculations from the response of this historic structure led to the following conclusions:

- Backhoe and jackhammer activity within a few meters of the structure did not create significant ground motions, which were less than 6mm/s (0.25 ips).
- Long-term environmental crack displacement was 20 to 60 times greater than the crack displacement caused by the largest measured construction-induced ground motion of 5 mm/s (0.21 ips).
- Crack displacements produced by occupant activity were larger than the largest construction vibration-induced crack displacement by a factor of 2 to 16, but smaller than the long-term environmental or weather induced crack displacement.
- The crack in the exterior stucco experienced larger long-term or weather-induced displacements (222 μm or 8880 μin) than either the molding crack (287 μm or 11500 μin) or plaster and lath crack (140 μm or 5600 μin).
- On-site inspection of vibration-inducing construction activities would diminish the difficulty in identification of specific sources of excitation.
- Electrical noise, human sources and other unidentifiable activities may trigger the system while monitoring construction vibrations.
- Cracks responded the most to ground motion with frequencies in the vicinity of 12 Hz, and much less to motions with frequencies around 45 Hz.
- There is no apparent correlation between outside humidity and rainfall level.

References

Dowding, C.H. (1996). Construction Vibration, Prentice Hall, Upper Saddle River, NJ.

Siebert, R.Damian (2003). Autonomous Crack Comparometer, M.S. Thesis, Department of Civil and Environmental Engineering, Northwestern University, Evanston, IL.

McKenna, L.M. (2002). Comparison of Measured Crack Response in Diverse Structures to Dynamic Events and Weather Phenomena, M.S. Thesis, Department of Civil and Environmental Engineering, Northwestern University, Evanston, IL.

Snider, M.L. (2003). Measurement and Analysis of Weather and Geodynamic Excitation-Induced Crack Displacements from Blasting in Connecticut and Construction Equipment in Las Vegas, M.S. Thesis, Department of Civil and Environmental Engineering, Northwestern University, Evanston, IL.

Petrina, M. (2004), Standardization of ACM apparatus for Long-Term Commercial Application, M.S. Thesis, Department of Civil and Environmental Engineering, Northwestern University, Evanston, IL.

Somat Ease version 3.0 (1999). Somat Corporation, Champaign, IL.

Somat TCE eDAQ, version 3.7.2 (2002). Somat Corporation, Champaign, IL.

Somat TCS for Windows, version 2.0.1 (1999). Somat Corporation, Champaign, IL.

APPENDIX A

DONUT METHOD FOR QUALIFYING LVDT'S

Introduction

Before LVDT (Linear Voltage Differential Transducers) are used on site to measure long-term micro inch crack response, it is essential to ensure in the laboratory that they operate properly. For that purpose, the testing procedure described below can be employed to determine the consistency of sensor performance through the definition of the hysterisis, drift, and noise level encountered with typically variable temperatures.

While other theses (i.e. Patrina, 2004) have addressed instrument qualification by attachment to a plate subjected to temperature variation, this procedure eliminates the plate in favor of a plastic donut between the sensor and the target (normally on the other side of the crack). This donut procedure allows a check on the plate procedure and is simpler to follow.

Any instrument that must endure cyclic temperature and humidity over long periods of time must maintain a constant relation between its output and the parameter being measured. Thus it cannot drift or have a large hysteretic response. Furthermore its noise level must be less than typical variations of the parameter being measured. Before proceeding it is important to define these three parameters with respect to measurement of micro inch crack displacement.

When a system, such as an LVDT sensor is placed across a crack, subjected to cyclic environmental changes over time (as occur inside and outside of structures) it should have a small hysterisis. Hysterisis is the difference between voltage output when the displacement is increasing and when it is decreasing over the same temperature range during one cycle. Figure A-1 illustrates large (a) and small (b) hysterisis where displacement (Data) varies temperature over time.

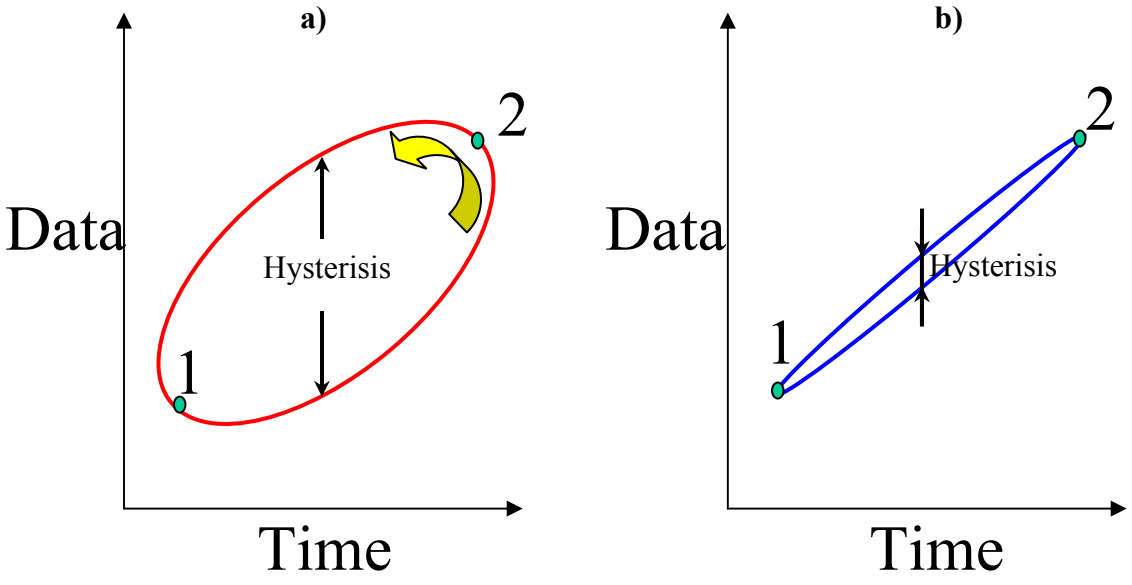

Figure A-1: Illustration of Hysterisis during a temperature cycle, showing a) poor and b) good performance.

It is also important that there be no to little instrument drift when crack response to cyclic environmental change is constant during each cycle as shown in Figure A-2 b). Drift is the variation of the sensor response (data) over time as is shown in Figure A-2. The only "drift" with time should be that of the crack.

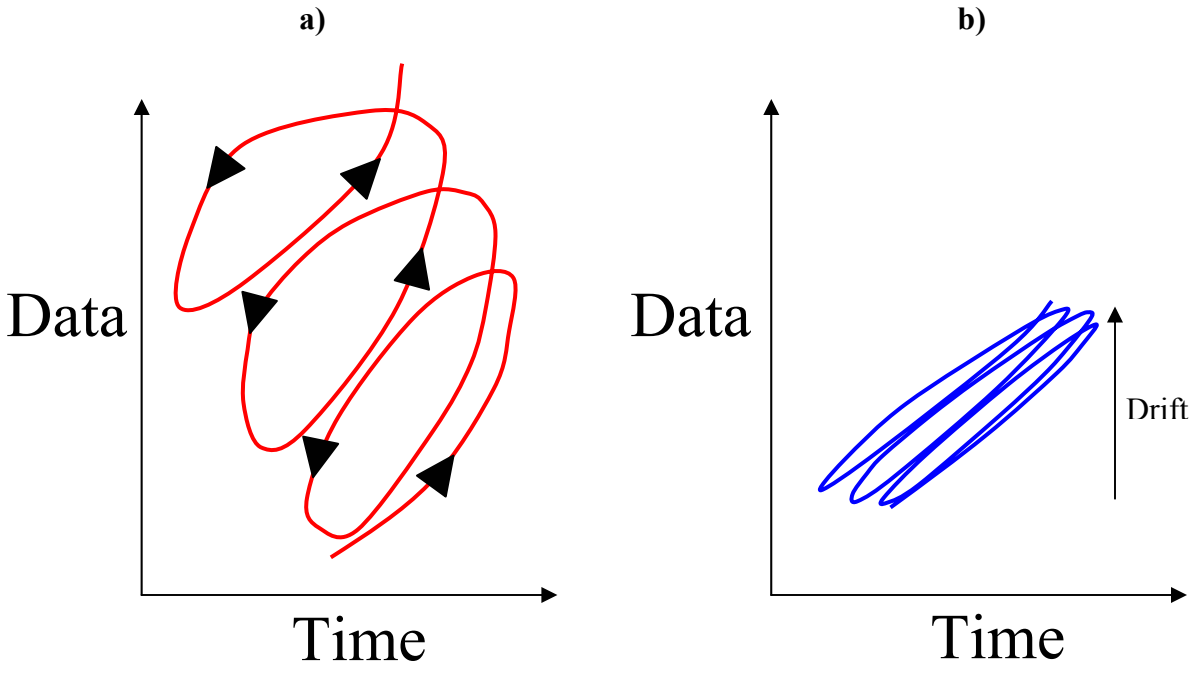

Figure A-2: Illustration of Drift during temperature cycles showing a) poor and b) good performance.

When crack displacements (data) are small the instrument noise level (or variation) shown in Figure A-3 must be smaller than the data trend over time as shown. In addition, the stair step analog to digital conversion resolution should be similar or less than the noise level.

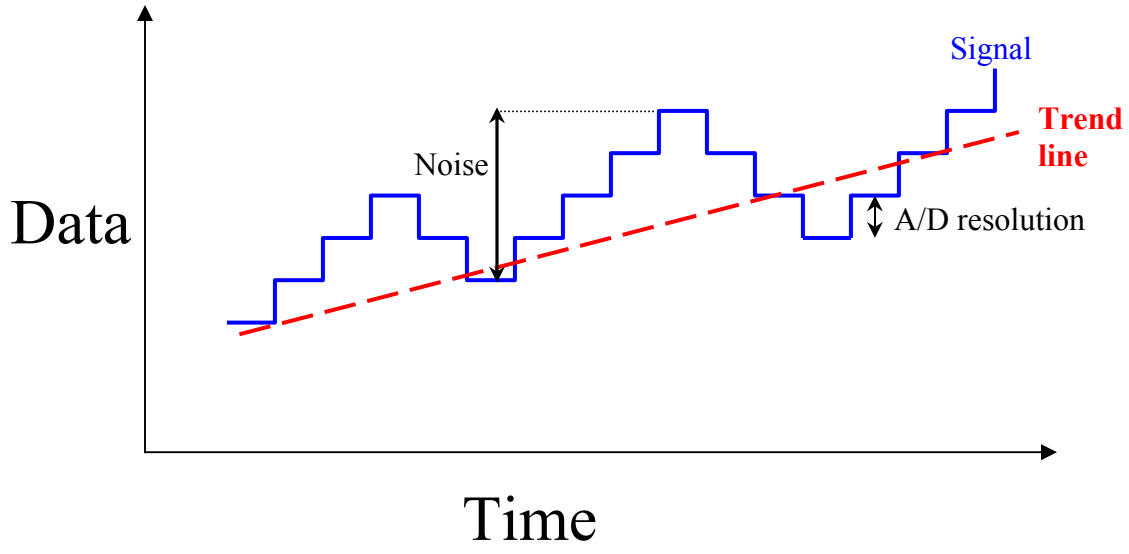

Figure A-3: Illustration of Noise during temperature variation.

Experimental setup and Hardware

Donut test configuration

As Figure 1 shows, the "LVDT Donut" configuration is composed of three visible parts: the coil, the plastic donut, and the bracket. The plastic donut was epoxied between the coil and the bracket. The LVDT rod which connects the bracket to the magnet inside the coil is inside the donut. The screw connection can be seen in the line drawing portion of Figure 1. The 1.27 cm (0.5 in) donut is machined from Ultra-High Molecular Weight Polyethylene (UHMW-P), also known as "poor man's Teflon". Its coefficient of thermal expansion (CTE, noted α) is relatively high, with a value of 198 $\mu m/m/^oC$ (110 $\mu in/in/^oF$). This high CTE value produces relatively large expansion and contraction with normal temperature fluctuations as discussed below.

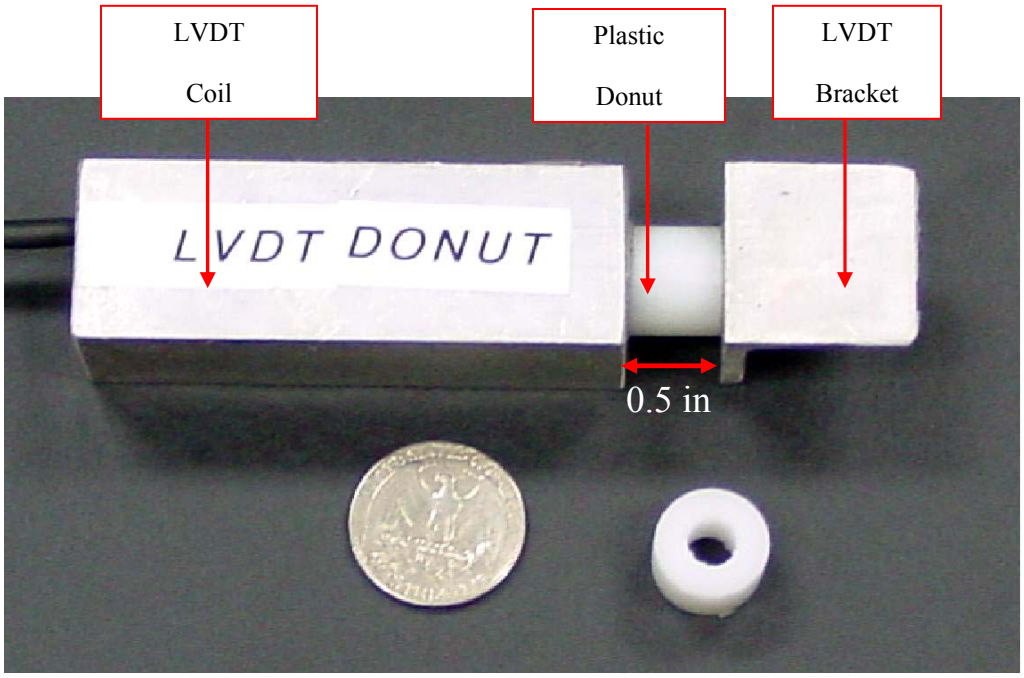

(a)

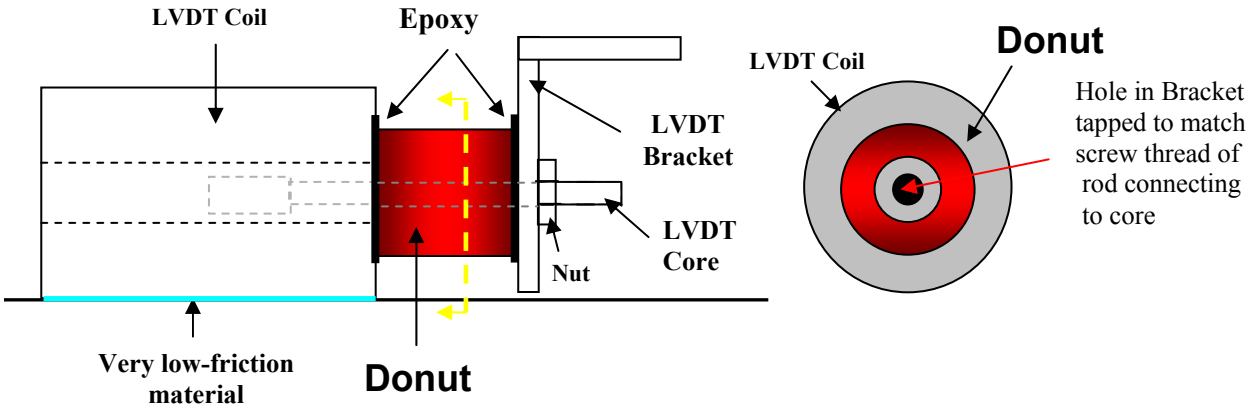

(b) (c)

Figure A-4: LVDT-donut components (a) quarter comparison, (b) side view, (c) front view

Plate test configuration

Figure 2 shows the configuration of the plate tests, which were conducted along with the donut test. Plate tests incorporated a SOMAT 2100 Field computer system data logger, a SOMAT 2100 Multiplexer, a "plate LVDT", a "donut LVDT", two temperature sensors, an LVDT power supply and a plate. Each component will be described in further detail below. The LVDT donut is placed on a plastic CD box in order to minimize the friction forces between the LVDT and the material on which it rests. To allow further comparisons in the results, the length of the donut (1.27 cm or 0.5 in) is also the length between the LVDT bracket and coil attached to the plate.

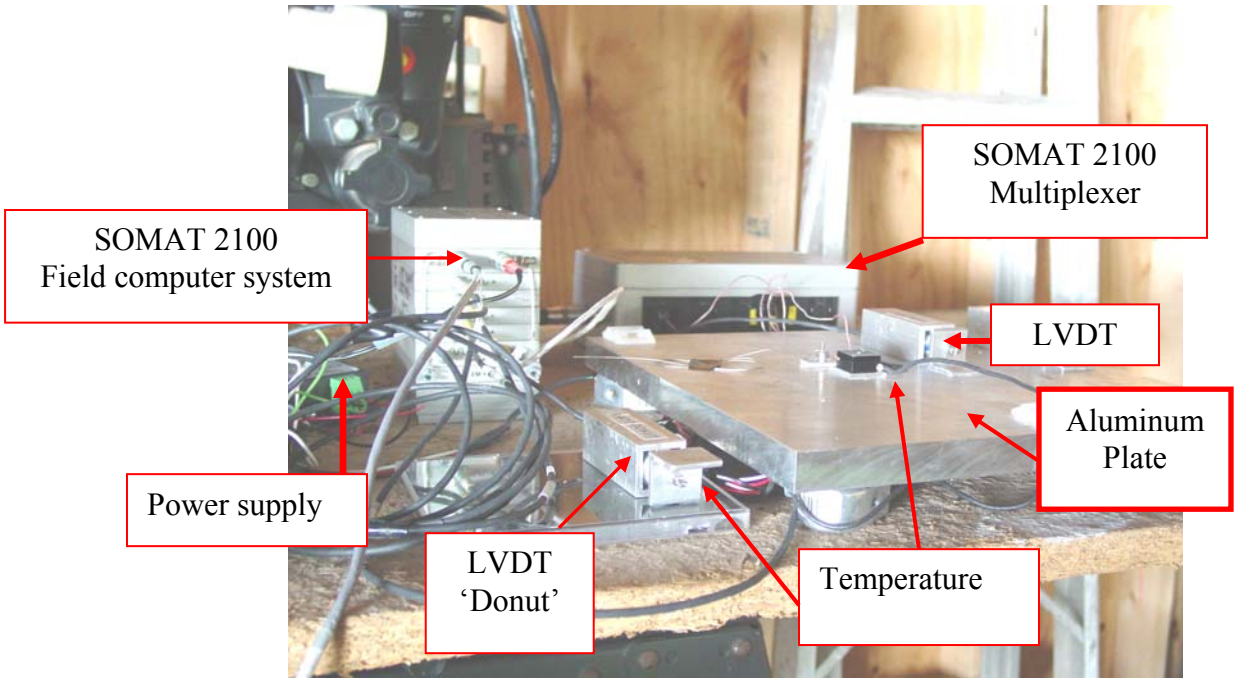

Figure A-5: Configuration of aluminum plate test and components

Plates were constructed of two different materials: Aluminum plate and UHWM-P with CTE's of 24μm/m/^{o}C (13 μin/in/^{o}F) and 198 μm/m/^{o}C (110 μin/in/^{o}F) respectively. The photograph in Figure 2 and 3 show the two plates. Both plate tests incorporated the same hardware components; the only difference between the two tests is the material of the plate. The plastic plate allowed a comparison of the two qualification approaches. Both the donut and plate were the same expansive material, with the same 1.27 cm (0.5 in) donut thickness and gap between the bracket and coil of the LVDT. Plate dimensions were 46cm/61cm/2cm (18''/24''/0.75'') (cost of 35$) and 30cm/30cm/2cm (12''/12''/0.75'') (cost 150$) for the plastic and aluminum plate respectively.

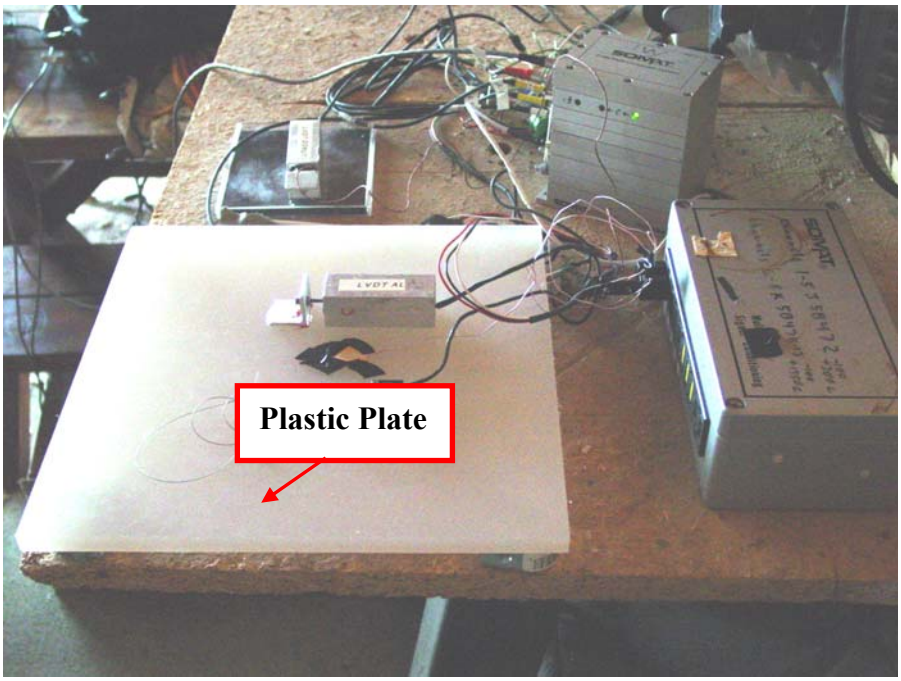

Figure A-6: Configuration of plastic plate test and components

Instruments and Hardware

An LVDT measures the expansion/contraction between coil/core and bracket. As the material between the coil and bracket on which the LVDT is mounted expands and contacts, the LVDT core moves back and forth inside the LVDT coil, producing a variable voltage output. LVDT's were epoxied to the plates along their full length. See Petrina (2004) for a detailed discussion of the comparison of full and partial gluing as well as "hot glue" vs epoxy.

For both experiments, a Macrosensors DC-750-050 "infinite resolution" LVDT served as the base-line system. They were powered with a regulated, linear –15 to +15 volts power supply, and sent output signals to the logger via a junction bridge. The loggers full scale range was set between –0.5 to +0.5 volts to reach an appropriate resolution for the test. This range resulted in a resolution of 0.031 μm (1.2 μin) with the 12 bit A/D converter.

All sensors were wired to the SOMAT data acquisition system, for controllably recording output voltage. By definition, the system resolution is the number of incremental steps into which the data logger's Analog to Digital (A/D) converter can divide the data. The data logger's 12 bit capability was able to subdivide the voltage range into $2^{12} = 4096$ steps.

The resolution in millivolts is calculated as the chosen voltage range divided by the A/D steps described above. In this case the resolution would be $[0.5 – (-0.5)]$ V / 2^{12} = 0.244 mV per A/D step. In other words, 0.244 mV is the smallest voltage variation the system will detect. The volts must be converted to μm with a conversion factor which in this case is 127 μm/V. Thus the A/D unit resolution times the conversion factor yields the

displacement per A/D unit, or 127 μm/V * 0.244 mV = 0.031 μm. In other words the smallest displacement the system will be able to detect is 0.031 μm, small enough for the purposes of this test.

The SOMAT 2100 stores up to 4MB of data. Typical data files were approximately 1.5 to 2MB in the proprietary SOMAT format. Data download was made through a serial cable to a laptop PC, which took typically 10 to 15 minutes to transfer. SOMAT proprietary software was employed to program the data loggers and to download and perform analysis of the data. Setting up and downloading the 2100 was accomplished with SOMAT TCS (version 2.0.1); the corresponding SOMAT software was SOMAT TCE-eDAQ (version 3.7.2). SOMAT has since developed more recent versions for both packages. SOMAT WinEase accomplished the data export from text files to Excel and MATLAB. SOMAT Infield now supersedes SOMAT WinEase.

Two thermocouple sensors were employed to measure temperatures of the expansive material. One was taped on the plate near the LVDT bracket and the other one was taped directly on the donut. The donut temperature sensor was bent around the cylinder-shaped donut in order to record the temperature of the plastic and not the air surrounding of the donut. These temperature sensors had a resolution of 0.2^{o}C, sufficient enough to obtain continuous data. Thermocouple voltage signal is converted to logger format in a 2100-compatible SOMAT Multiplexer. The two temperature sensors were wired to the SOMAT 2100 multiplexer, (the metallic box at the rear in Figure 2), which in turn was attached to the SOMAT.

Results

Plate apparatii shown in Figures 2 and 3 were placed in an enclosed but unheated garage where the temperature gradually increased and decreased on a 24 hour cycle more than would occur inside a residential structure.

Long-term data responses were recorded each hour. Averages were computed for groups of 1000 points obtained every hour. Data were digitized at a rate of 1000 Hz, so 1000 points would be obtained in one second. These average values obtained hourly in one second were transferred to Excel for manipulation and displayed with Grapher. Once data were transferred to the PC and saved in a text file format, they were processed with a Matlab program.

Figure A-7 compares response of LVDT's to thermally induced natural expansion/contraction. Both material and measurement instruments system were subjected to the gradually changing temperature environment shown on the bottom half of the figure. In the top half, the right and left sides compare responses of the LVDT when epoxied to an aluminum (left) and plastic plate (right). Both LVDT responses (black) are compared to responses induced by donut expansion/contraction (blue) during that time.

There is a constant difference of approximately $5^{o}C$ ($23\ ^{o}F$) between the donut and plate temperature. The LVDT coil is constantly energized and generates heat with the passage of an electric current, and the plastic donut with lower thermal mass and close proximity to the heat source is much more affected than the plate. In other words, the massive aluminum plate dissipates heat it receives from the LVDT much faster than the donut, which is too small and to close to the LVDT to dissipate the heat energy

efficiently. Despite this difference in thermal condition, the daily temperature fluctuation is very nearly the same.

There are a number of observation that can be made from Figure A-7

- Plastic produces a larger displacement per degree temperature change, which is similar to the expansion experienced by system spanning crack in typical wall materials.
- The air temperature ranged between 16 ^{o}C and 30^{o}C (61^{o}F and 86^{o}F), which is more than the span of typical indoor temperatures (60 ^{o}F to 75^{o}F).
- Temperatures cycled daily as would occur in the field, and thus any drift or hysteresis could be observed.
- The LVDT installed on a plastic plate experienced greater displacement than did the donut although the distance between the coil and the bracket was the same.
- This difference in donut and plate response is equivalent to adding 50 μm (200 μin) distance between the coil and the bracket.

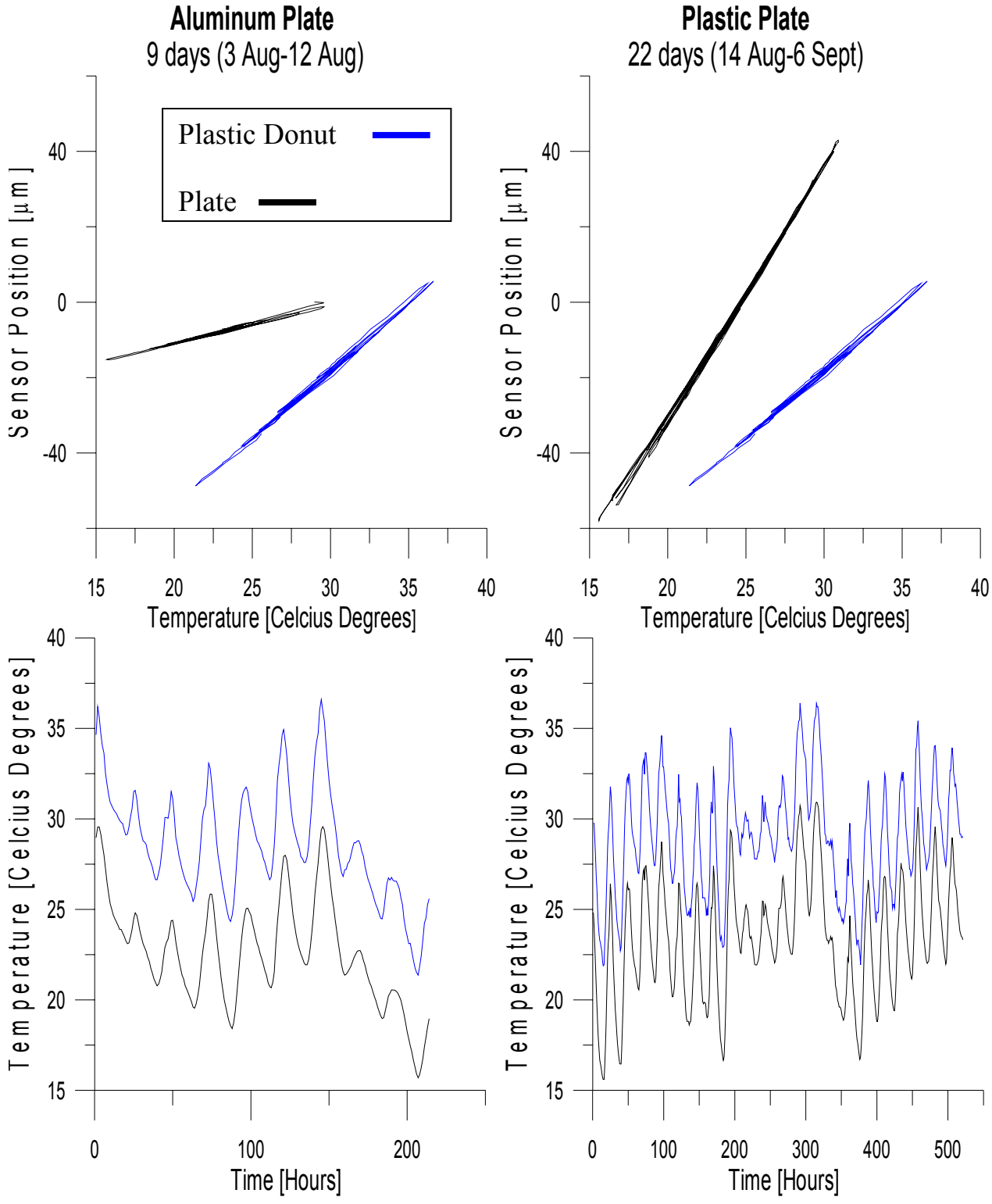

Figure A-7: Comparisons of LVDT responses to thermally induced when attached to plates (aluminum or plastic) or donuts.

Discussions and Conclusions

Figure A-8 compares the "donut" and plate results in terms of the agreement of measured and calculated displacements. Measured displacements are found directly from the instrument voltage and conversion factor. Calculated displacements are computed via the thermal expansion equation below. As with Figure A-7, the aluminum plate results are presented on the left graphs and the plastic plate results are presented on the right.

Calculated displacement, δ, is computed from temperature with the formula $\delta = \alpha * L * \Delta T$, where α is the coefficient of thermal expansion of the material (plate or plastic donut), L the length of the donut and ΔT the temperature difference. One temperature and one LVDT position data point are available for each hour for each displacement sensor. From these data are computed the calculated cumulative displacements in micrometers. The cumulative displacements are path related. Calling T_i the temperature at hour *i*, starting from T_0, the calculated cumulative displacement at time t is equal to $D_t = \alpha * L * (T_t - T_0)$. T_0 is the reference point for the calculated cumulative displacement.

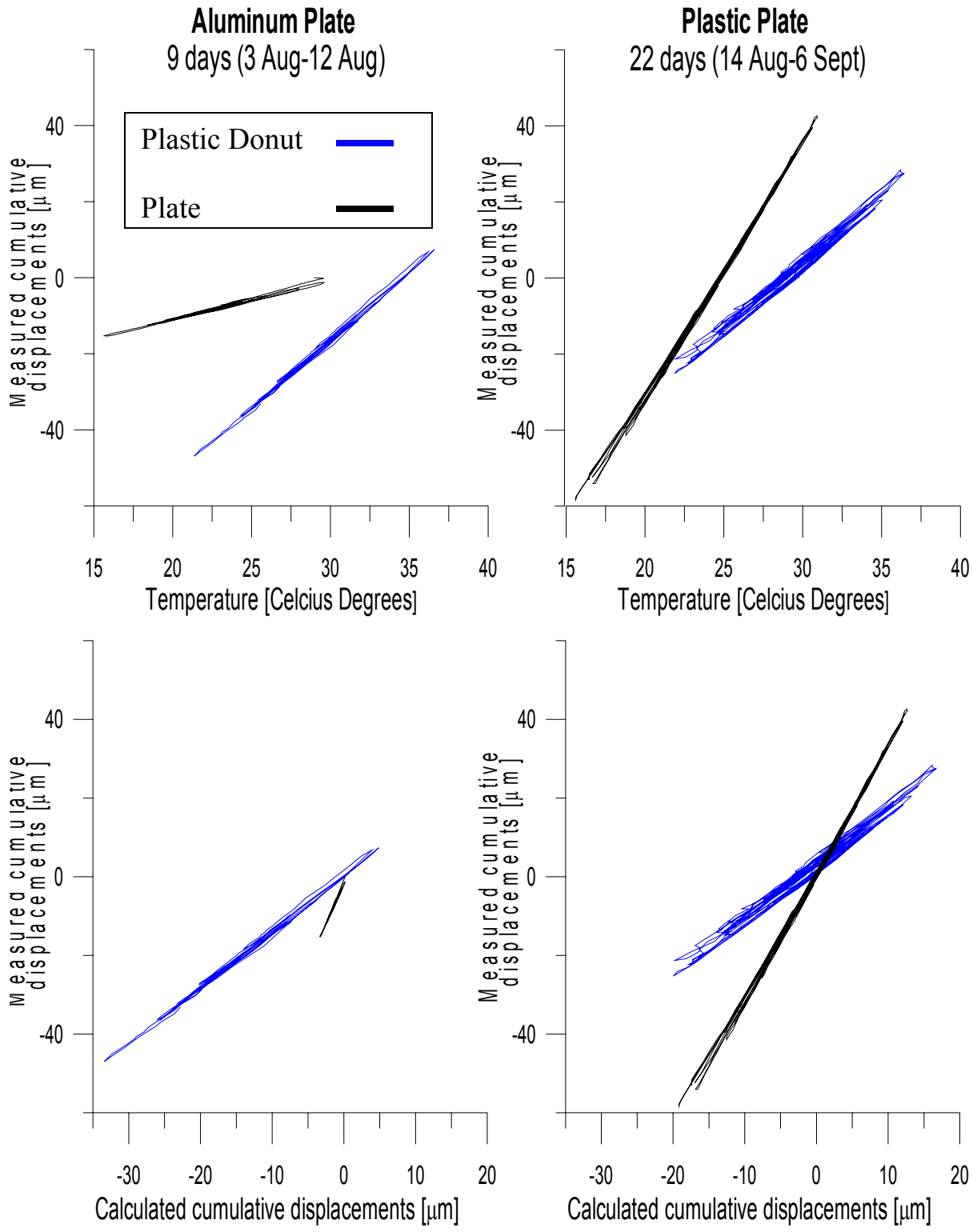

Figure A-8: Comparisons of measured and calculated LVDT responses for the aluminum or plastic plate and plastic donut installation.

Plate Type	Time [days]	LVDT_DONUT				LVDT_PLATE			
		coeff_1	coeff_2	σ	R^2	coeff_1	coeff_2	σ	R^2
Plastic	22	0.013	0.010	0.486	0.995	0.004	0.003	0.330	0.999
Aliminum	9	0.013	0.010	0.419	0.994	0.023	0.015	0.181	0.981

Table A-1: Time and amplitude of resolution of data

Statistics of the variability of measured vs. calculated displacement are summarized in Table A-1. In Table A-1, coeff_1 is equal to the residual mean over the difference between the two extreme values of the measured cumulative displacements, whereas coeff_2 is equal to the standard deviation of the measured cumulative displacements (with respect to the regression line), divided by the difference between the two extreme values of the measured cumulative displacements. These ratios are defined below, with MCD standing for Measured Cumulative Displacements:

Coef_1= [Residual Mean of MCD]/[Largest MCD Variation]

Coef_2= [Standard Deviation of the MCD]/[Largest MCD Variation]

Comparison of donut response to the plastic and aluminum plate responses differ. For the plastic plate test comparison (top row in Table A-1) all LVDT Donut coefficients are larger than for the LVDT Plate. In other words the donut data are more spread out around their trend line than are the plate data as is obvious from Figure A-8. On the other hand, compared to the aluminum plate test, the donut coefficients are smaller than for the LVDT plate. This reversal is due to the fact that the relative hysterisis of the loops for the aluminum plate displacements although small are not smaller compared to the difference in the extreme values of the measured displacement.

The crucial question becomes, is the spread or combination of hysterisis and drift of the instrument as defined by either the donut or plastic plate test sufficiently small. Some sense of the answer can be obtained by comparison with the long term response reported in the main body. Figure 4-11 shows that the daily weather changes induce crack displacement of 150 μm, and 30 or 25 μm for the exterior and two interior cracks respectively. The maximum weather effect produced by the passage weather fronts induces crack displacements of 75 to 200 μm. The maximum spread of the "measured" donut and plastic plate displacement from the 22-day qualification test in Figure A-8 are only 5 and 2 μm respectively.

Thus it appears that no matter how the qualification test is conducted, the spread in the qualification displacements is 15 to 40 times smaller than weather front induce crack displacement.

Figure A-9 is a plot of a two-day portion of the graph in Figure A-8. Two days of data imply two loops, which is enough to display the typical drift, hysterisis and noise level. The two frames at the bottom are expansions of the colored frames on the upper graph. In those frames the red arrows indicate the first loop, whereas the blue ones indicate the second loop, and the green dot by the red arrows indicate the first loop direction. As the two lower frames show, there was little drift or hysterisis. The loops are tight and occur is the same space with little divergence. As the frames show the noise level is also very low as the measured displacement ranges between –35 and 10 μm while the A/D resolution is 0.031 μm.

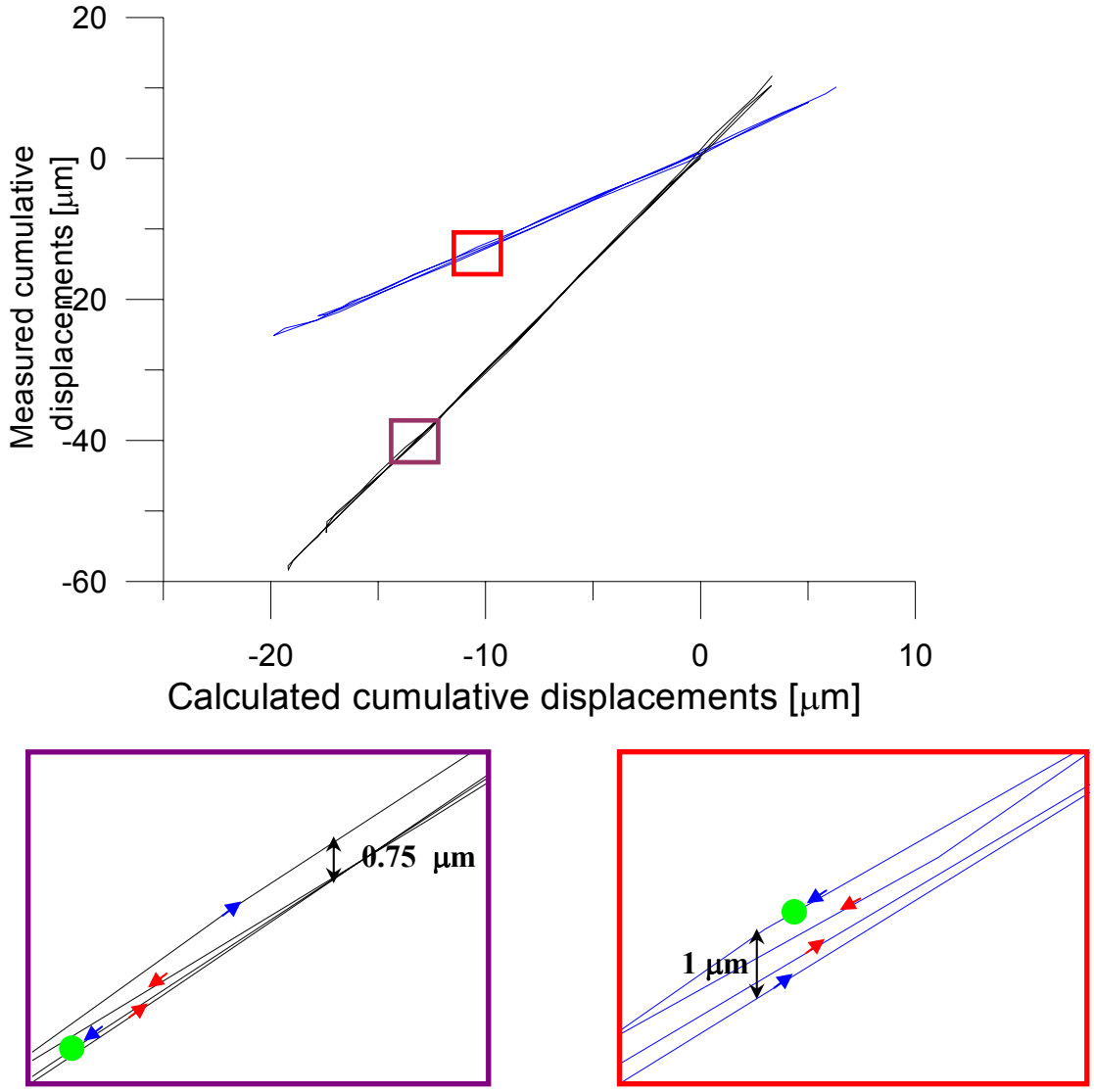

Figure A-9: Expansion of two daily loops of temperature induced expansion and contraction from Figure A-8.

Even though plate displacement is larger than donut displacement this observation is not detrimental to the approach. In other words for a same material, the plate displacement exceeds the donut displacement with the same length of material between core and bracket. Suppose the LVDT reports crack (C) plus wall material and gauge (G) response to be C+G (=X). Then the real crack response would be X-G. But G is too large by ΔG (the difference between the plate (G) and donut responses (D) as shown in Figure A-10), thus the corrected response would be X- (G- ΔG) which is X+ ΔG-G and greater than X-G. Thus the real crack change is greater than thought and the X-G value is conservative.

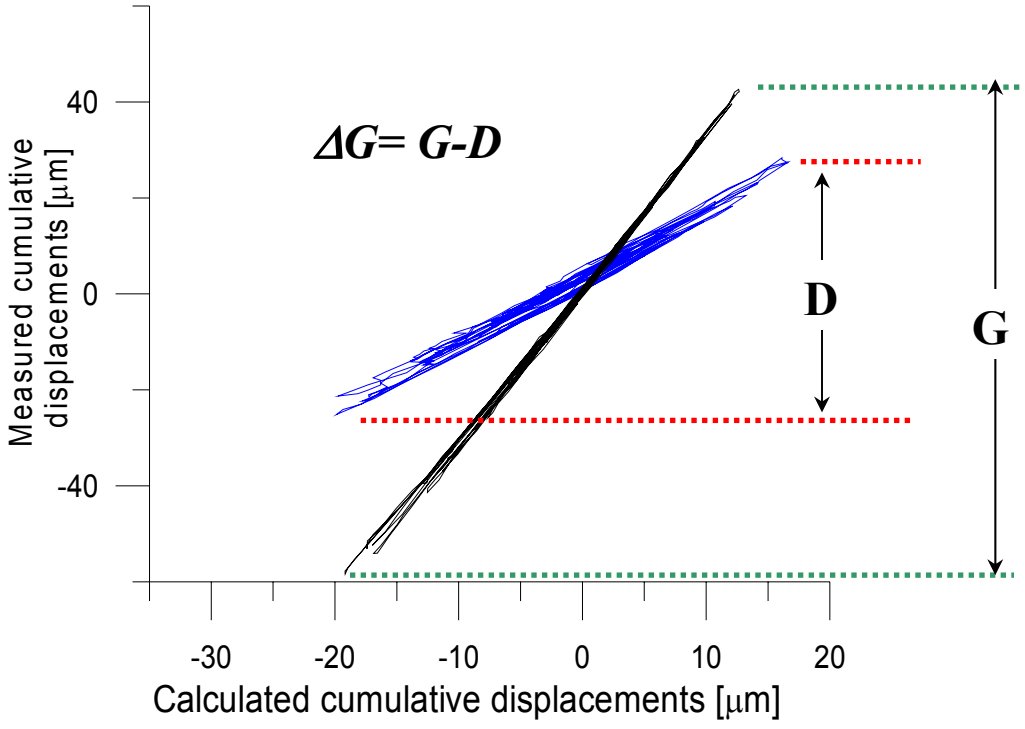

Figure A-10: The difference ΔG between plate and donut response

APPENDIX B

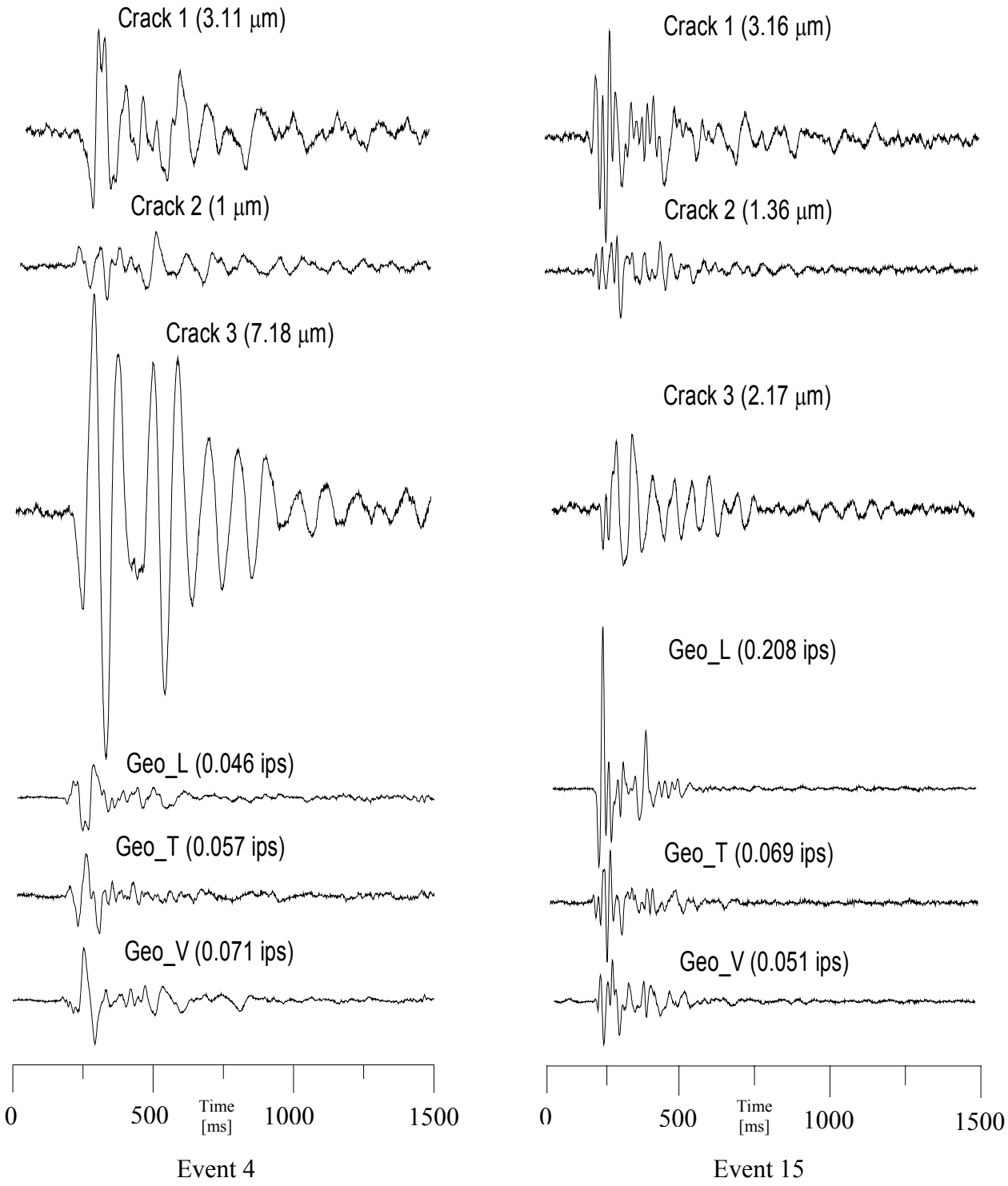

Figure B-1: Event 4 and 15 who induced largest crack 2 and 3 displacements (Figure 4-11).